Available online at www.sciencedirect.com
ScienceDirect
Precambrian Research 158 (2007) 228–262
Precambrian Research
www.elsevier.com/locate/precamres

Diverse microstructures from Archaean chert from the Mount Goldsworthy–Mount Grant area, Pilbara Craton, Western Australia: Microfossils, dubiofossils, or pseudofossils?

Kenichiro Sugitani [a,*], Kathleen Grey [b,c], Abigail Allwood [c,1], Tsutomu Nagaoka [d], Koichi Mimura [e], Masayo Minami [f], Craig P. Marshall [c,g], Martin J. Van Kranendonk [b,c], Malcolm R. Walter [c]

[a] *Department of Environmental Engineering and Architecture, Graduate School of Environmental Studies, Nagoya University, Nagoya 464-8601, Japan*
[b] *Geological Survey of Western Australia, Department of Industry and Resources, 100 Plain Street, East Perth, WA 6004, Australia*
[c] *Australian Centre for Astrobiology, Macquarie University, Sydney, NSW 2109, Australia*
[d] *School of Informatics and Sciences, Nagoya University, Nagoya 464-8601, Japan*
[e] *Department of Earth and Environmental Sciences, Graduate School of Environmental Studies, Nagoya University, Nagoya 464-8601, Japan*
[f] *Nagoya University Center for Chronological Research, Nagoya 464-8602, Japan*
[g] *School of Chemistry, The University of Sydney, Sydney, NSW 2006, Australia*

Received 7 February 2007; received in revised form 16 March 2007; accepted 16 March 2007

Abstract

A diverse assemblage of indigenous carbonaceous microstructures, classified here as highly probable microfossils to pseudomicrofossils, is present in the >ca. 2.97 Ga Farrel Quartzite (Gorge Creek Group) at Mount Grant and Mount Goldsworthy, Pilbara Craton, Western Australia. The microstructures are an integral part of the primary sedimentary fabrics preserved in black chert beds. The interbedding of chert with layers of large silicified crystal pseudomorphs and fine to coarse grained volcaniclastic/clastic beds indicate deposition in a partially evaporitic basin with terrigenous clastic and volcaniclastic input.

Similar associations of microstructures are present at the same stratigraphic level in outcrops more than 2 km apart. Four major microstructural types are present: thread-like, film-like, spheroidal and lenticular to spindle-like, each of which can be further subdivided into several sub-types. Most of the microstructures were deposited as part of an assemblage of chemical and clastic sediments, although there are some thread-like microstructures present for which a synsedimentary origin cannot be confirmed. Many specimens appear to have originally had flexible but breakable walls and some occur in colony-like aggregations. Size distributions for the four major types are generally narrow, a feature typical of biogenic structures. The microstructures are composed of disordered carbon (as revealed by Raman spectroscopy) and the bulk isotopic composition of the carbon is $\delta^{13}C < -30$ per mil, which is consistent with biological processing.

The combined morphological and geological evidence suggests that the film-like structures, small spheres associated with films, large spheroids and spindle-like structures are probable to highly probable fossil remains of microorganisms. The morphological variety among the microstructures suggests that a diverse microbial ecosystem flourished in the Pilbara region during the Archaean.
© 2007 Elsevier B.V. All rights reserved.

Keywords: Archaean; Pilbara; Microfossil; Farrel Quartzite; Chert; Evaporite

* Corresponding author. Tel: +81 527894865; fax: +81 527894865.
E-mail address: sugi@info.human.nagoya-u.ac.jp (K. Sugitani).
[1] Current address: NASA Jet Propulsion Laboratory, 4800 Oak Grove Drive, Pasadena, CA 91109, United States.

0301-9268/$ – see front matter © 2007 Elsevier B.V. All rights reserved.
doi:10.1016/j.precamres.2007.03.006

1. Introduction

Microscopic structures resembling fossilized microorganisms in Archaean rocks may be the only true fossil remnants of Earth's first inhabitants. However, the biogenicity of most, if not all, structures previously interpreted as Archaean microfossils (e.g., Awramik et al., 1983; Knoll and Barghoorn, 1977; Schopf and Packer, 1987; Schopf, 1993; Walsh and Lowe, 1985, also see Schopf, 2006 and references therein) has been questioned (Buick, 1984, 1988, 1990; Altermann, 2001; Brasier et al., 2002, 2004, 2005, 2006; García-Ruiz et al., 2002, 2003). The controversy centres around evidence that natural abiotic processes may replicate both the biological morphology (García-Ruiz et al., 2003) and biological composition (Holm and Charlon, 2001; van Zuilen et al., 2002; McCollom, 2003; McCollom and Seewald, 2006; Lindsay et al., 2005) of microbial remains. Thus, morphological and compositional criteria widely used to identify Phanerozoic and some Proterozoic fossils have been discredited or considered insufficiently rigorous for the most ancient rocks, and there is currently no universally accepted test for biogenicity. Many problems associated with interpretation of microfossils in Archaean rocks arise from their occurrence in geologic settings such as hydrothermal veins (Ueno et al., 2004; Lindsay et al., 2005; Van Kranendonk, 2006), which generate conditions known from laboratory simulations to produce abiotic organic compounds with light isotopic compositions (McCollom, 2003; McCollom and Seewald, 2006). Others emerge from ambiguities in geological context, which raise questions about the processes of formation of the structures. Relatively few Archaean microfossils have been identified in well-characterized bedded sediments (e.g., Westall et al., 2006), and it has been stated that there are, as yet, no Archaean structures that have been unequivocally demonstrated as biological in origin (Brasier et al., 2005; Moorbath, 2005).

In this paper, we examine a newly discovered population of abundant, morphologically diverse, carbonaceous microstructures from bedded cherts of the Archaean (>ca. 2.97 Ga) Farrel Quartzite in the Gorge Creek Group at Mount Goldsworthy and Mount Grant in the East Pilbara Terrane of the Pilbara Craton, Western Australia. The Mount Grant and Mount Goldsworthy microstructures are investigated using a multidisciplinary approach in the light of recent and historical advances in the analysis of microfossil-like structures, and are presented as a case study for exploring and developing constructive palaeontological methods for microfossil analyses.

We document the geological context, composition, morphological variability, and relationships between the Mount Grant and Mount Goldsworthy microstructures to assess evidence for biogenicity. From field observations, petrography, morphological analysis, inorganic geochemistry, and organic geochemistry the microstructures are classified as microfossils, dubiofossils or pseudofossils (Hofmann, 1971, 1972), following criteria for biogenicity proposed by Schopf and Walter (1983), Buick (1990), Schopf and Klein (1992), Hofmann (1994, 2004 and personal communication, 2006), Westall and Folk (2003) and Brasier et al. (2005).

2. Geological setting

The microstructures occur in black chert beds that outcrop along the southwest-trending ridges of Mount Grant and Mount Goldsworthy, approximately 100 km east of Port Hedland in the East Pilbara Terrane. The East Pilbara Terrane, which formed between 3.52 and 3.19 Ga, is one of five lithotectonic terranes, unconformably overlain by the De Grey Superbasin, which make up the Pilbara Craton (Fig. 1a). The East Pilbara Terrane contains a thick stratigraphic succession comprising the 3.52–3.43 Ga Warrawoona Group; the 3.43–3.31 Ga Kelly Group; the 3.27–3.24 Ga Sulphur Springs Group; the ca. 3.24–3.19 Ga Soanesville Group; the unconformably overlying ca. 2.99–2.93 Ga De Grey Supergroup (Van Kranendonk et al., 2007).

At Mount Grant and Mount Goldsworthy, Gorge Creek Group sedimentary rocks are locally thicker than 1 km and lie unconformably on strongly altered volcanic and volcaniclastic rocks of the Warrawoona and Kelly Groups of the East Pilbara Terrane (Smithies et al., 2004; Sugitani et al., 2006c,d). In the study area (Zones I and III in Fig. 1b, Sections 1, 2 and 4 in Fig. 2), the Gorge Creek Group comprises a lower clastic unit, the Farrel Quartzite (previously, Corboy Formation; see below), and an upper cherty unit, the Cleaverville Formation (Smithies et al., 2004; Van Kranendonk et al., 2006, 2007). At eastern Mount Grant (Zone II in Fig. 1b, Section 3 in Fig. 2), the Farrel Quartzite is missing, although a thin sandstone layer less than 1m thick is present and the Cleaverville Formation appears to directly overlie the Warrawoona Group (Fig. 1b). There are no distinct structural discontinuities between Zone II and the others, implying that the sedimentary succession of this region includes a contemporaneously deposited deep basinal facies (Zone II) and shallow coastal facies (Zones I and III) (Sugitani et al., 2003).

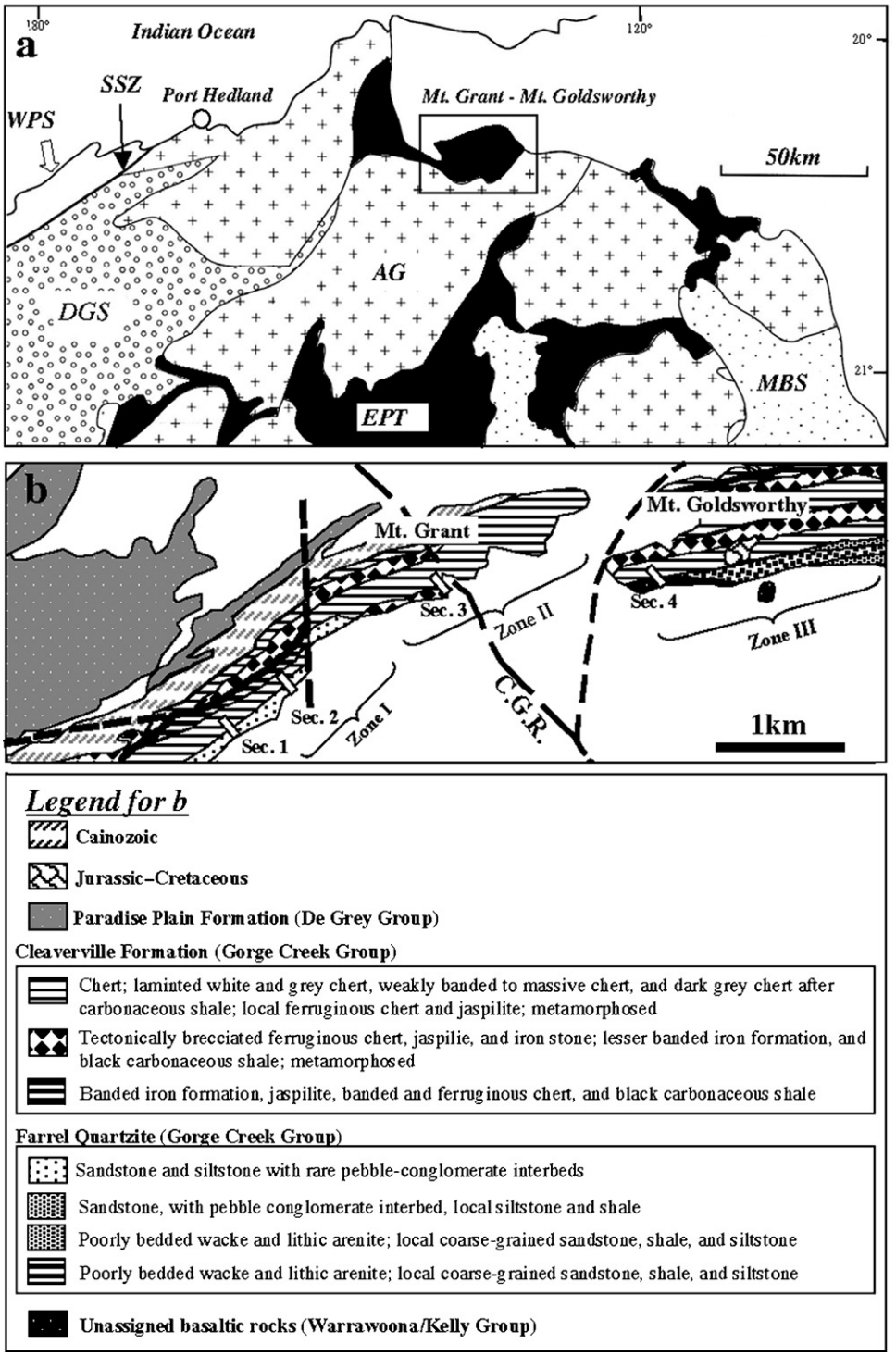

Fig. 1. (a) Geology of north-eastern part of the Pilbara Craton (after Smithies et al., 2004). WPS, West Pilbara Superterrane; SSZ, Scholl Shear Zone; DGS, De Grey Superbasin; AG, Archaean granitoid rocks; EPT, East Pilbara Terrane; MBS, Mount Bruce Supergroup; Ph, Phanerozoic cover. (b) Local geology of Mount Goldsworthy and Mount Grant (after Smithies et al., 2004 and Van Kranendonk et al., 2006, 2007). CGR, Coongan-Goldsworthy Road. Thick dashed line shows fault.

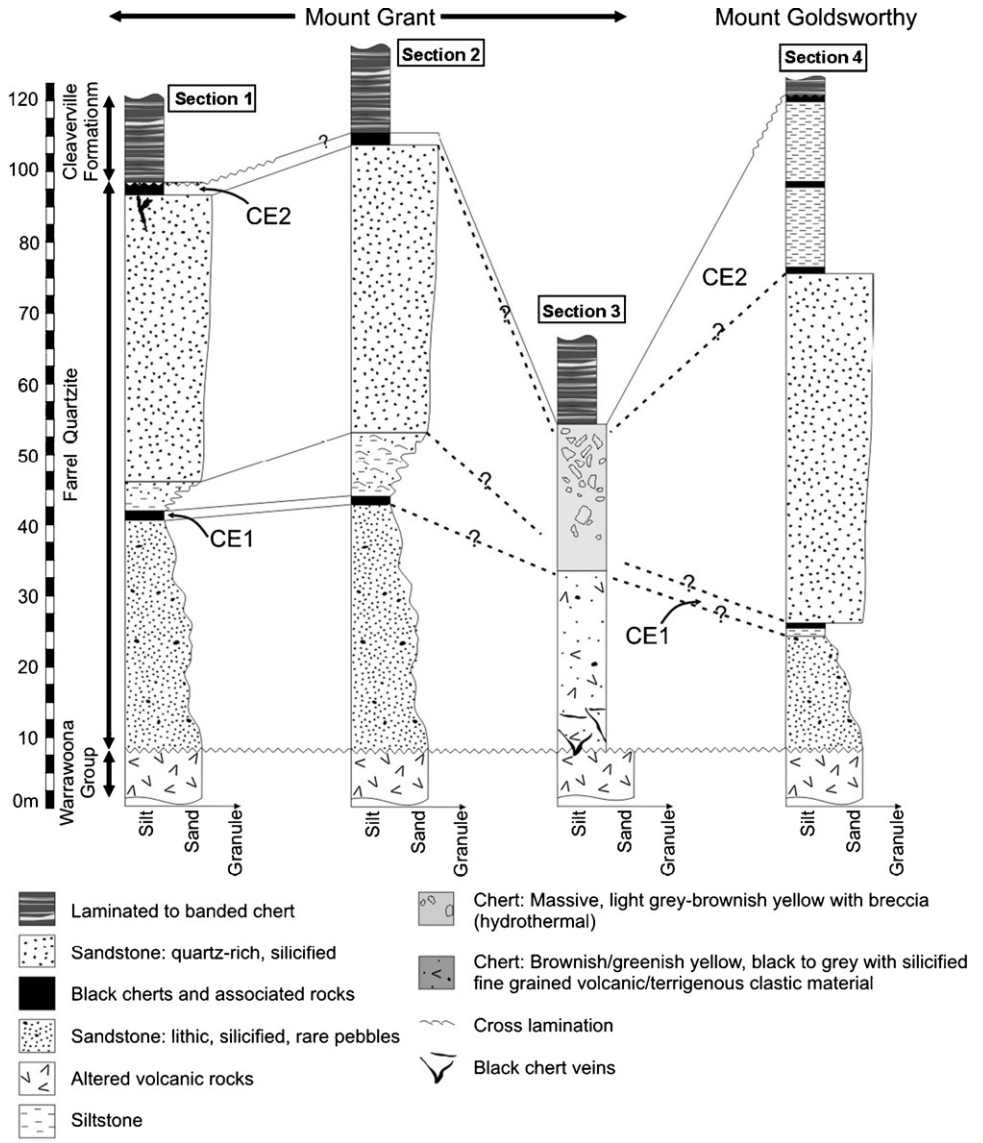

Fig. 2. Stratigraphic correlation for the four sections at Mount Goldsworthy and Mount Grant. Also see Fig. 1b for locations of the sections.

Although Sugitani et al. (2006a,b,c,d) previously suggested that part of the sedimentary succession might belong to the Strelley Pool Chert (Lowe, 1983), the black chert beds described here have been mapped as being near the top of the Corboy Formation, lower Gorge Creek Group, basal De Grey Supergroup (Smithies et al., 2004), but were subsequently redefined as Farrel Quartzite (also lower Gorge Creek Group) (Van Kranendonk et al., 2006). In the East Pilbara Terrane, the age of the Gorge Creek Group is geochronologically constrained by the ages of the underlying Soanesville Group (ca. 3.19 Ga) and the overlying Croydon Group (ca. 2.97 Ga) (Van Kranendonk et al., 2006, 2007). On the western margin of East Pilbara Terrane (Nunyerry Gap area, GSWA sample 142842), the Cleaverville Formation of the Gorge Creek Group was dated at ca. 3.02 (Van Kranendonk et al., 2007).

3. Stratigraphy and facies of the Farrel Quartzite

The Farrel Quartzite lies along the southern slopes of Mounts Grant and Goldsworthy and comprises predominantly quartz-rich sandstone with minor conglomerate and beds of pseudomorphed evaporitic minerals with mafic volcaniclastic layers and several thin black chert layers (Figs. 2–5). Three zones, Zone I (containing Sec-

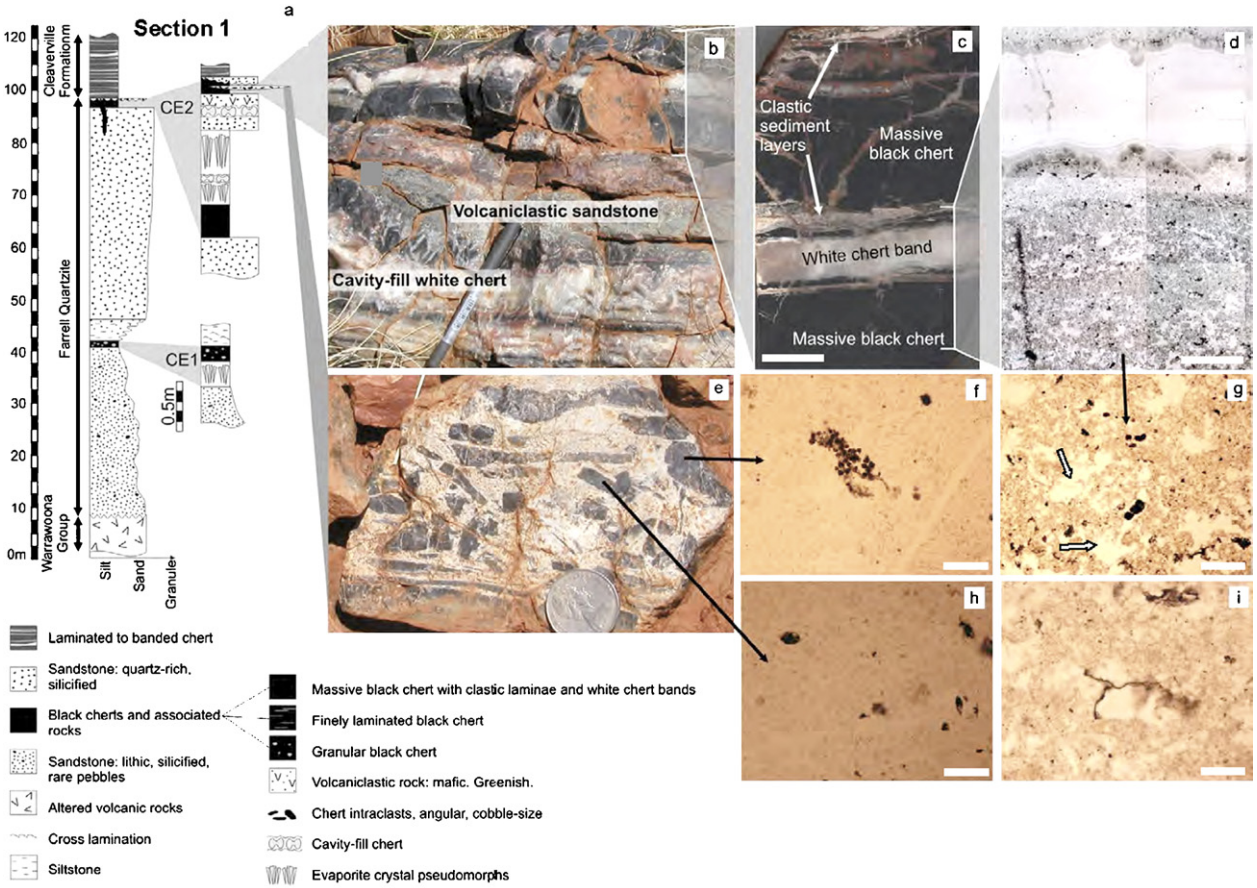

Fig. 3. Stratigraphy and petrography for Section 1 (West Mount Grant, Zone I, see Fig. 1b) (a) Stratigraphic column. (b) Photograph of representative outcrop. (c) Photograph of polished slab of black chert layer enriched in microstructures. Scale bar: 2 cm. (d) Composite figure of photomicrograph of massive black chert, with white chert band displaying colloform texture. Irregularly shaped chert masses are common in massive black chert. Scale bar: 1 mm. Note that size of chert masses tends to be smaller in the middle part of massive chert. (e) Black chert breccia. Chert clasts are set in the sandstone. (f) and (h) Examples for microstructures in chert clasts of (e). Scale bars: 100 μm. (g) and (i) Examples for microstructures in massive black chert in (d). Scale bars: 100 μm. White arrows in (g) show irregularly shaped chert masses. Four hand specimens (ORW4B, NORW1, NORW2 and NORW4) were collected from CE2, for key palaeontological analyses.

tions 1 'West Mount Grant' and 2, 'Middle Mount Grant'), Zone II (containing Section 3, 'East Mount Grant') and Zone III (containing Section 4, Mount Goldsworthy) can be identified from west to east, based on lateral variations in facies and lithology, and the succession is further subdivided into lower and upper units (Figs. 1–5).

Sugitani et al. (2003, 2006c) interpreted the succession as a continental margin deposit containing terrigenous detrital materials partially derived from granitoid rocks. The microstructures described here are found in the upper part of the sections in unit CE2 in Sections 1, 2, and 4 (Figs. 3–5). Of these, the most complete section is Section 1 at Mount Grant.

3.1. 'West and Middle Mount Grant': Zone I, Sections 1 and 2

Farrel Quartzite is present at the western and middle part of Mount Grant (Figs. 1b and 2; Sections 1 and 2). The section consists of: 20 m of sandstone with abundant lithic fragments; overlain by approximately 8 m of dark-coloured, clastic sedimentary rocks with local cross-lamination and chert breccia; overlain by up to 50 m of coarsening-upward quartz-rich sandstone with minor conglomerate and chert (Figs. 2–4). Two black chert/evaporite horizons (CE1 in the lower part of the formation and CE2 in the upper part of the formation) are present in Zone I and are correlated with CE1 and CE2,

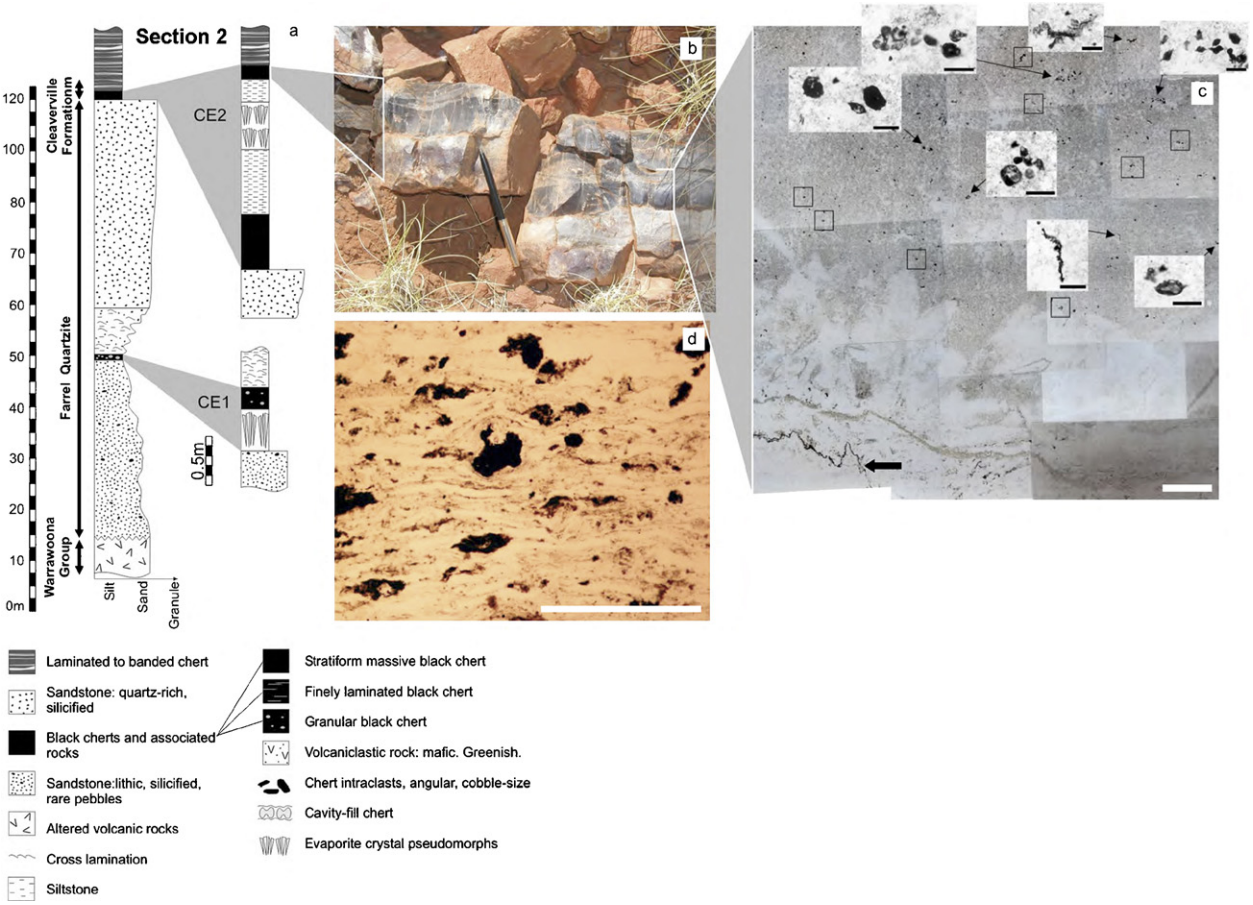

Fig. 4. Stratigraphy and petrography for Section 2 (Middle Mount Grant, Zone I, see Fig. 1b). (a) Stratigraphic column. (b) Photograph of the stratiform massive black chert containing microstructures and underlying clastic layer. (c) Composite figure of microphotographs of black chert, with abundant randomly distributed microstructures. The thick arrow shows the boundary with the underlying clastic layer, where a stylolite is developed. In the lower half of this figure, silicified prismatic crystals are abundant. Scale bar: 1 mm. Representative microstructures are indicated by squares and smaller photographs at higher magnification (scale bars: 50 μm). (d) Photomicrograph for the black chert in CE1, which is characterized by parallel fine lamination and/or composite grains of carbonaceous matter. Scale bar: 500 μm. For palaeontological analyses, one hand specimen (GFWE3) was collected from CE2.

respectively, at Mount Goldsworthy (Zone III). Both the upper and lower black chert-evaporite associations are laterally extensive (i.e., around 2 km). In CE1, a black chert layer ca. 30 cm thick directly overlies a 50-cm thick evaporite bed (Fig. 3). The upper chert-evaporite association (CE2) consists of inter-bedded stratiform black chert, clastic sediments (including quartz-rich sandstone and mafic volcaniclastic rocks) and two beds of evaporite crystal pseudomorphs (Fig. 3a and b). In the uppermost part of CE2, the black chert is locally brecciated, with chert breccia clasts in a sandstone matrix (Fig. 3e). Black chert veins are extremely rare, and are present only locally in the uppermost portion of the quartz-rich sandstone where small (~10 cm wide) veinlets cross-cut (and post-date) the sedimentary succession. The microstructures predominantly occur in CE2 black cherts, and are particularly abundant in the uppermost black chert layer, whereas they are absent in CE1. Only thread-like microstructures can be seen in vein chert.

3.2. *'East Mount Grant': Zone II, Section 3*

The Farrel Quartzite is obscured (or possibly absent) at 'East Mount Grant'. The basal part of the succession comprises ~20 m of chaotically mixed, varicolored, massive cherty rocks. This is overlain by hydrothermally brecciated chert, with a thin sandstone layer and then laminated to banded chert of the Cleaverville For-

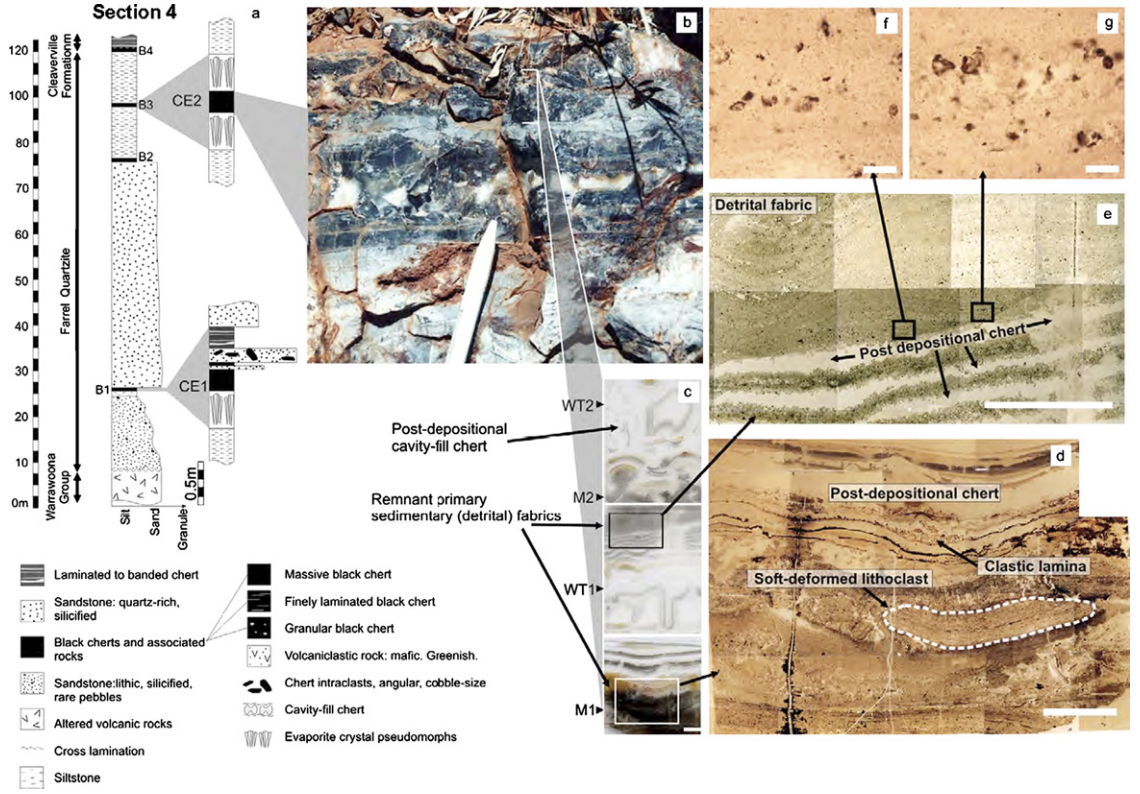

Fig. 5. Stratigraphy and petrography for Section 4 (Mount Goldsworthy, Zone III, see Fig. 1b). (a) Stratigraphic column. (b) Representative outcrop of stratiform massive black chert containing microstructures, with brecciated clastic laminae (light grey) and white to translucent chert lithology characterized by stalactitic texture. This chert is underlain by fine-grained clastic rock. (c) Composite figure of scanned images of thin sections of black chert equivalent to the black chert in (a) (WT, white to translucent chert; M, massive chert). Reddish-brown altered (oxidized) portion contains hematite and goethite particles. Scale bar: 5 mm. (d) Composite figure of black chert characterized by soft sediment deformation. Scale bar: 5 mm. (e) Composite figure of black chert characterized by lamination that is composed of microstructures. Scale bar: 5 mm. (f) and (g) Magnification of lamination in (e). Scale bar: 100 μm. For palaeontological analyses, two hand specimens (GWM11A and NGWM1) were collected from CE2. (For interpretation of the references to color in this figure legend, the reader is referred to the web version of the article.)

mation (Fig. 2, Section 3). Black chert is present in the Cleaverville Formation and locally as a thin layer and dyke less than 20 cm thick within the varicoloured chert.

3.3. Mount Goldsworthy: Zone III, Section 4

At the western end of Mount Goldsworthy, the Farrel Quartzite consists of bedded, silicified, quartz-rich sandstone and shale, with two horizons (CE1 in the lower part of the formation and CE2 in the upper part of the formation) (Figs. 2 and 5) containing siliceous crystal pseudomorphs and thin layers (less than 30 cm thick) of black chert. The stratigraphic succession readily correlates with the Mount Grant succession. At Section 4 (Fig. 5), CE1 consists of layered black chert immediately above a bed of large (~40 cm) vertically to sub-vertically oriented siliceous crystal pseudomorphs. The crystals are interpreted as replacement after evaporitic nahcolite (Sugitani et al., 2003). The black chert is partially interbedded with sandstone that contains tabular black chert clasts and silicified detrital and authigenic barite grains, indicating a primary origin for both the chert and barite. CE2 lies in the upper part of the formation and consists of a black chert layer interbedded with two layers of large (~40 cm) vertically to sub-vertically oriented siliceous crystal pseudomorphs (Fig. 5a), equivalent to those in CE1. The microstructures occur predominantly in CE2; only very ambiguous microstructures have been found in black chert in CE1. Minor black chert is present throughout the succession as: (1) thin discontinuous layers (less than 10 cm) in the uppermost part of the succession (B4) and at ca. 15 m below CE2 (B2) (Fig. 5a); (2) local, heterogeneous replacement chert among some of the evaporite crystal pseudomorphs. There are no black chert feeder veins associated with any of the black chert beds.

4. Samples and methods

4.1. Sample collection and handling

Samples collected in 2001 and 2003 from the black chert in CE2 (Fig. 2) consisted of eight hand specimens (ORW4B, NORW1, NORW2, NORW 4 from Section 1 at 'West Mount Grant', and GWM11A, NGWM1, NGWM2, NGWM3 from Section 4 at Mount Goldsworthy) and provided key palaeontological, petrographic and chemical analyses; details of other specimens and supplementary information are given in figure captions. Hand specimens were cut into several slabs, mostly perpendicular to bedding and thin sectioned for microscopic studies or used for microanalyses. The remainder was crushed into millimeter-sized fragments and hand picked fragments (20–30 g), free of alteration and secondary mineral phases, were ultrasonically cleaned in de-ionized water, powdered using an agate mill, and subjected to organic and inorganic geochemical analyses.

Hand-specimens and thin sections are currently in the collection at Nagoya University, Japan, while studies continue. They will eventually be reposited in an Australian collection as required under the Australian Protection of Movable Cultural Heritage Act.

4.2. Microscopic analyses

Microscopic analyses were initially performed for basic petrography, but after the discovery of the microstructures, further analyses were carried out to determine morphological information, including the three-dimensional shape and distribution of the microstructures, and size data using standard petrographic thin sections (2.4 cm × 3.4 cm wide and 30–35 μm thick). Preliminary examination of 80 thin sections, using a petrographic microscope (Olympus BH2), was followed by systematic traversing at a magnification of 1000× using a Leitz-DMPR transmitted-light microscope of sixteen selected thin sections from Mount Goldsworthy. Microstructure positions were recorded using an England Finder (see figure and appendix captions). The prefix R- or L- indicates the label position.

4.3. Organic geochemistry

4.3.1. Raman spectroscopy

Raman analyses were performed in order to establish the carbonaceous composition of the microstructures and the crystallinity of the carbon. Representative Raman spectra (Fig. 8a) were collected in situ from polished thin sections containing individual carbonaceous microstructures; spectra were acquired on a Renishaw Raman Microprobe Laser Raman Spectrometer using a charge coupled detector in The University of Sydney. Details of equipment and analytical conditions can be found in Marshall et al. (2007).

4.3.2. Elemental and isotopic analyses

Elemental compositions (C, H, N and S) and carbon isotopes of organic matter (residues obtained by HF and HCl digestion) were analyzed in order to obtain basic information about thermal maturation and source of organic matter.

Powdered chert samples were digested with concentrated HF and HCl. Residual opaque materials were subjected to elemental analyses (N, C, H, and S) using Fisons EA1800. For the carbon isotopic analyses, residual materials were further treated with heavy liquids and organic matter was purified. The organic matter obtained through the chemical procedures described above was combusted at 850 °C in a sealed Vycor tube containing CuO and Ag wires. The CO_2 gas was purified cryogenically. The carbon isotope ratio was measured using a Finnigan MAT-252 analyser. The $\delta^{13}C$ values are given in conventional δ-notation in the PDB scale. Precision was 0.1 per mil.

4.4. Major elements and C, H, N and S

Major elements were analyzed using an automatic X-ray fluorescence spectrometer (XRF) (Shimadzu SXF-1200) using fused-glass discs made from a mixture of powdered sample and flux ($Li_2B_4O_7$) in the proportion of 1:5 (Sugisaki et al., 1977). Elemental compositions of bulk samples were also analyzed using an elemental analyzer.

4.5. Microanalyses of constituent minerals

Microanalyses of constituent minerals were performed with SEM-EDX analyzer (JEOL840A, equipped with Oxford ISIS2000) in Osaka Prefecture University, using ZAF method for qualitative analyses, in order to identify some minerals.

5. Sedimentology and petrography of the microstructure-bearing black chert and microstructure occurrences

The origin of chert is a fundamental issue in constraining the origin of any microfossil-like structures and organic matter it contains (e.g., Brasier et al., 2005; Lindsay et al., 2005; Tice and Lowe, 2004). Different

types of chert include: precipitated sedimentary chert, non-sedimentary, chemically precipitated vein or cavity-fill chert; cherty rocks formed by replacement of other rock types (e.g., Buick and Dunlop, 1990; Lowe, 1999; Sugitani, 1992; Sugitani et al., 1998). Each carries implications about the possible origins of any microstructures they contain. For example, abiotic hydrothermal processes can produce microstructures with seemingly biological morphology and carbonaceous materials with seemingly biological isotopic composition, stimulating skepticism about the biological origins of 'microfossils' found in hydrothermal vein systems. The cross-cutting nature of veins also introduces ambiguity regarding the age of any microstructures. In addition, the criterion that a microfossil must occur in a geological setting that is viable for life (e.g., Hofmann, 1994) means that – although microbes are known to exist in the deep subsurface (e.g., Gold, 1999) – they are common in surface environments and therefore microfossils found in surface deposits may be less equivocal with respect to this criterion. We therefore pay particular attention to determining whether the microstructure-bearing stratiform black cherts studied herein are primary sediments deposited at the Earth's surface in the Archaean, as opposed to bedding-parallel chert 'sills' that appear superficially like chert beds (Nijman et al., 1998). We also pay attention to determining whether the microstructures occur within parts of the strata that were not formed through diagenetic alteration (Brasier et al., 2002, 2004, 2005).

5.1. Sedimentology and petrography of black chert

The microstructure-bearing black chert layers (CE2) are conformable, even locally interbedded, with the surrounding sandstones and evaporite crystal pseudomorph-rich beds (Figs. 2–5) and are traceable for 2 km along strike at Mount Grant and are present at Mount Goldsworthy, 4.5 km further east (Figs. 1–5). They also locally contain thin layers of fine-grained clastic sediment (Figs. 3c and 5b), and occur as brecciated clasts in sandstone (Fig. 3e). This indicates that the microstructure-bearing black chert layers are not cross-cutting, post-depositional sills, but were deposited as part of the original sedimentary succession.

Although patches and layers of white to translucent chert with agate-like or stalactitic cavity-fill texture are present (discussed below) (Figs. 3b–d and 5b, c), the black chert layers generally have a massive fabric. This contrasts with some bedded cherts in other parts of the formation (e.g., CE1), which have laminated and granular fabrics (Figs. 4d and 6a, b). In thin section, the black chert is composed of a microcrystalline quartz matrix with disseminated carbonaceous material. Thin layers of terrigenous clastic and volcaniclastic material, and silicified prismatic crystals also occur (Figs. 3c, 4c). Additional minor components in the chert include sulfide (mostly pyrite), an unidentified acicular crystal (possibly a silicate), with minor barite and carbonate. Sulfide grains and aggregates tend to be concentrated within specific layers. Most of the spheroidal sulfide ranges from 5 to 15 μm in diameter, whereas aggregates and euhedral grains are (rarely) >100 μm in diameter.

Distributed carbonaceous matter varies in different parts of the black chert. In parts, the chert is characterized by a fabric of very fine carbonaceous particles that tend to be distributed heterogeneously around irregularly shaped pure chert masses of various sizes (Fig. 3g (arrowed) and i). These pure chert masses display simultaneous (non-random or domain) extinction, a feature typical of re-crystallized chalcedony (Simonson, 1985). The surrounding carbonaceous chert shows random extinction. The size, shape and distribution pattern of the pure chert masses varies but they tend to be spatially and stratigraphically controlled, as seen in Fig. 3d. Elsewhere in the chert, remnant patches of laminated sedimentary fabric, defined by very fine carbonaceous particles and microstructures, are preserved. (Fig. 5e–g). The fabrics imply sorting of sedimentary detritus in the water column, thereby indicating deposition at the sediment/water interface.

Silicified carbonaceous lithoclasts occur locally in the black chert, and appear to be the same lithology as the rest of the black chert bed. Some of the clasts are tabular whereas others are curviplanar, or "bent" (Fig. 5d), indicating soft-sediment deformation. The presence of the soft sediment intraclasts suggests that the black chert was deposited as a kind of carbonaceous, siliceous mud, and that it underwent synsedimentary reworking in the surface environment prior to full lithification.

Areas of white to translucent chert (Figs. 3b–d, 5b, c) in parts of the black chert bed are characterized by broad, white to translucent laminae and thinner, dark, particulate laminae less than 10 μm thick. White and translucent laminae are composed of nearly pure microcrystalline quartz, whereas dark laminae are enriched in minute carbonaceous particles. Agate-like or stalactitic texture is common in this type of chert (WT1 and 2 in Fig. 5c). The central part of this lithology is often filled with microcrystalline quartz masses showing a chalcedonic domain extinction figure, or mega-quartz mosaic with abundant fluid inclusions. Large sulfide grains and carbonate rhombs are locally present. A few thread-like microstructures occur in the white to translucent chert (see below).

Microstructures are present in the carbonaceous chert characterized by both a relatively massive fabric with irregularly shaped pure chert masses and by remnant laminated sedimentary fabrics. Moreover, microstructures are integral to laminated fabrics (Fig. 5e–g), implying that the microstructures were deposited along with other sedimentary detritus in a subaqueous surface environment.

5.2. Occurrence of microstructures

Distribution of the four major morphological microstructures (thread-like, film-like, spheroidal, and lenticular to spindle-like structures) is lithologically and stratigraphically controlled. First, most are restricted to the massive, stratiform black chert, although thread-like structures are also found in colloform vein chert and replacively silicified evaporite. At Mount Grant, microstructures are found in CE2 in Sections 1 and 2. Similar microstructural assemblages have been identified at several locations along strike. At Mount Goldsworthy, microstructures are present in massive black chert in the upper chert-evaporite association (CE2) and in the uppermost portion of the clastic unit (B4) and 15 m below CE2 (B2) (Fig. 5a). CE1 at Mount Goldsworthy also contains microstructures. Although poorly preserved, possible film-like structures can locally be observed in massive black chert in the lower chert-evaporite association.

No microstructures were found in laminated and granular black chert in CE1 at Mount Grant (Sections 1 and 2). Laminated chert in the lower part of the Mount Grant succession displays a distinctly different fabric to the microstructure-bearing black cherts in the upper part of the formation—with parallel to slightly undulating lamination, abundant detrital carbonaceous grains (Fig. 4d) and locally thin layers of fine-grained quartz and mica (Fig. 6a) and silicified prismatic crystals (Fig. 6b). These characteristics suggest a higher energy depositional setting that might have destroyed any microbial remains that might have been present.

Microstructures are also absent in black chert veins cross-cutting the Mount Grant succession (Fig. 2). A black chert vein, less than 10 cm thick and less than 5 m in length, cross cuts the uppermost sandstone bed. This vein is characterized by colloform structures, in which only some thread-like microstructures are found (Fig. 6c). A relatively large-scale black chert vein (dyke), 10–20 cm thick, occurs within chaotically mixed massive rocks at the base of the sedimentary succession in Zone II (Fig. 2). This chert dyke contains abundant composite grains of carbonaceous matter, with no microstructures (Fig. 6d). Carbonaceous black chert is found in the Cleaverville Formation (Figs. 1b and 2). The chert is characterized by fine parallel lamination without composite grains. This chert also contains no microstructures.

Fig. 4c shows a relatively well-preserved sample of microstructure-bearing black chert, in which silicified prismatic crystals form laminae and stylolites develop at the boundary with the underlying clastic layer. Abundant microstructures are present in the matrix, but not within the silicified crystals and underlying silicified clastic layer. Fig. 6e shows a heavily altered portion of massive chert. In this area, the microstructure-containing lithology has been subjected to every type of alteration such as bleaching (silicification), ferruginization and vein-intrusion. When microstructures have been found in these altered portions, they are bleached or ferruginized as well. Furthermore, the distribution pattern of microstructures is unaffected by altered fabrics in their vicinities.

5.3. Microtexture (spherulites) of host chert and its implications of chert origin and timing of embedding of microstructure

The microstructure-bearing chert matrix consists of microcrystalline quartz composed mainly of spherulites of variable (but usually about 5–10 μm) diameter, outlined by abundant, finely dispersed submicron carbonaceous particles (Fig. 7a) that tend to be concentrated around spherulite margins giving the matrix a lacey, reticulate appearance. The particles are rarely concentrated in sufficient quantities to appear as a solid structure, they appear more concentrated where seen in vertical view. Similar finely disseminated carbon particles in the Bitter Springs Formation chert (Schopf, 1968) and many Phanerozoic cherts, as well as other Archaean cherts, such as the Buck Reef Chert (Barberton Mountain Land, South Africa) (Fig. 7b) are usually interpreted as being the break-down products of organic material. Spherulite formation and the formation of rims of excluded impurities were demonstrated experimentally by Oehler and Schopf (1971) and Oehler (1976). They showed that chalcedonic quartz spherulites can form in primary chert directly from colloidal gel rather than by secondary replacement and that they tend to nucleate on the surfaces of organic matter. Spherulites are replaced by hexagonal quartz mosaic on recrystallization. The presence of spherulitic texture rather than hexagonal mosaic texture provides evidence for the primary nature of the chert matrix.

The finely disseminated particles that make up the tracery are physically (although not necessarily chem-

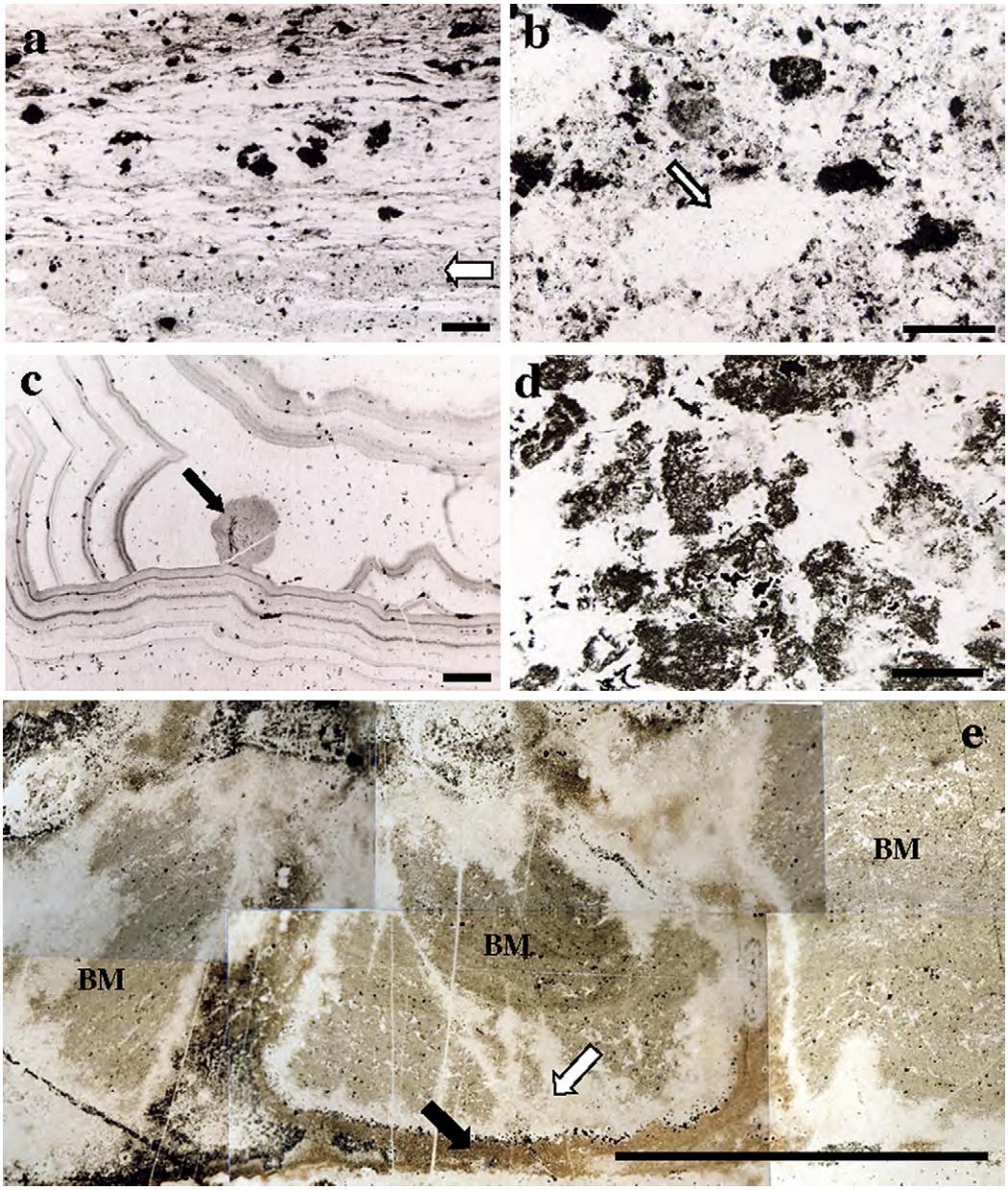

Fig. 6. Photomicrographs of various types of black cherts. Non-polarized light. Scale bar: 200 μm (a–d); 5 mm (e). (a) Laminated stratiform black chert containing carbonaceous composite grains. The arrow shows a clastic lamina. Sample from CE1 in Section 2 (see Fig. 4). (b) Composite grains of carbonaceous matter and associated silicified prismatic crystals (the arrow) in stratiform black chert collected from CE1 in Section 1 (see Fig. 3). (c) Colloform textured black chert vein in quart-rich sandstone just below CE2 at Section 1 (see Fig. 3). The arrow shows thread-like structures. (d) Carbonaceous clots in black chert dyke from the basal portion of Section 3 (see Fig. 2). (e) Heavily altered portion of stratiform massive black chert from Mount Goldsworthy (Section 4, CE2). BM shows unaltered portion, whereas the white arrow and solid arrow show silicified (bleached) portion and ferruginized portion, respectively. Some microstructures can be seen in BM.

ically) significantly different from the material that makes up the walls of the microstructures (Fig. 7). The relationships between the spherulites and many of the microstructures at different levels of focus and in transmitted and polarized light demonstrate that microstructures were present at the time the matrix crystallized, and were not introduced later. Microstructures can be traced through different focal depths in thin section, and are commonly cut by narrow quartz veins (Fig. 7a–d). Detailed study of the relationship between

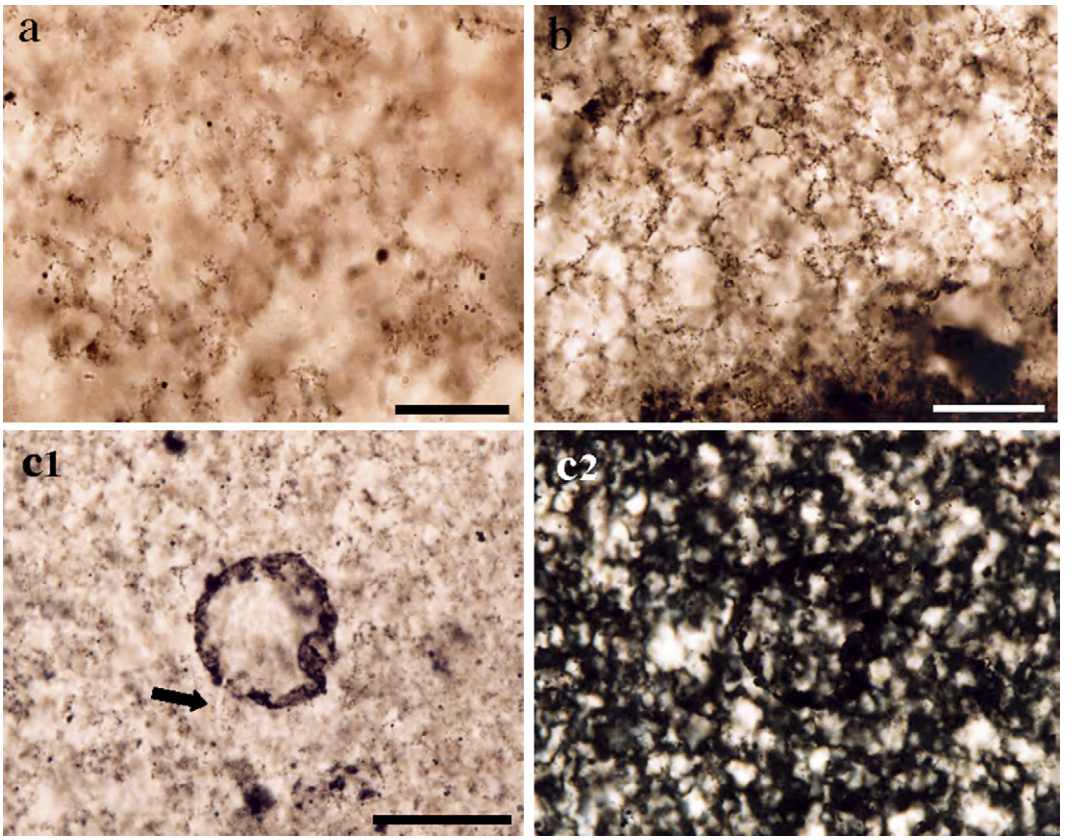

Fig. 7. Examples of primary spherulitic chert and a spherical microstructure in spherulitic chert. (a) Typical spherulitic chert from Mount Grant, Slide NGWM3. Scale bar is 20 μm. Spherules are outlined by finely disseminated carbonaceous particles to form a reticulate network. Spherules are variable in diameter, but about 5–10 μm in diameter. Note the circular structure of the spherulites and the very thin particulate matter margin (several levels of spherulites are visible in the field of view). (b) Similar spherulite pattern from the ca. 3.4 Ga Buck Reef Chert, Barberton Mountainland, South Africa. Scale bar is 20 μm. (c) A spherical hollow microstructure in spherulitic chert under transmitted light (c1) and polarized light (c2). SlideNGWM3, Position R-L37/3. Scale bar is 50 μm. Note the clear quartz centre in the spherulites and the more or less continuous solid margin to the sphere. The sphere is filled with spherulites similar to those in the matrix. Note the crosscutting veins (solid arrows) that indicate the prior formation of both the spherulites and the sphere.

carbonaceous microstructures and crystal boundaries indicates that most of the structures described in this study are not crystal bounded (Fig. 7c2). As discussed above, the primary chert crystallized as small, indistinct spherulites. Microstructure interiors may contain several spherulites and there is no evidence that the position of the microstructure walls is controlled by the distribution of the spherulites as suggested by Brasier et al. (2005) for the 'Apex Basalt chert'. Walls do not follow the contours of the spherulites as they would if they were formed by a secondary redistribution of particulate matter.

6. Carbonaceous composition and thermal maturity of microstructures

Raman spectra show that the microstructures of all morphological types are composed of carbonaceous matter. Reflective microscope and SEM-EDX analyses also show that the structures contain rare disseminated sulfide particles.

Fig. 8a shows a representative Raman spectrum acquired from carbonaceous microstructures. The two prominent bands in the carbon first-order region (900–1800 cm^{-1}) are assigned to the G (1600 cm^{-1}) and D (1343 cm^{-1}) bands, which correspond to graphite and disordered carbon, respectively (for details, see Marshall et al., 2007).

The intensities of the G and D bands with respect to one another can be used as an index of metamorphic alteration (e.g., Wopenka and Pasteris, 1993; Jehlicka et al., 2003 and references therein). The lineshape of the carbon first-order region correlate well with previous studies of carbonaceous materials from biotite metamorphic zones (e.g., Wopenka and Pasteris, 1993;

Jehlicka et al., 2003 and references therein) representing lower to mid greenschist facies (Yui et al., 1996), indicating peak temperatures between 400 and 500 °C (Bucher and Frey, 1994). No significant differences in relative intensities of the G with D bands can be seen between different morphological types and irregularly shaped carbonaceous clots in the matrix. Carbonaceous matter in the upper chert unit, in chert clasts in sandstone, and in dyke chert also shows similar D/(D + G) ratios (Fig. 8b).

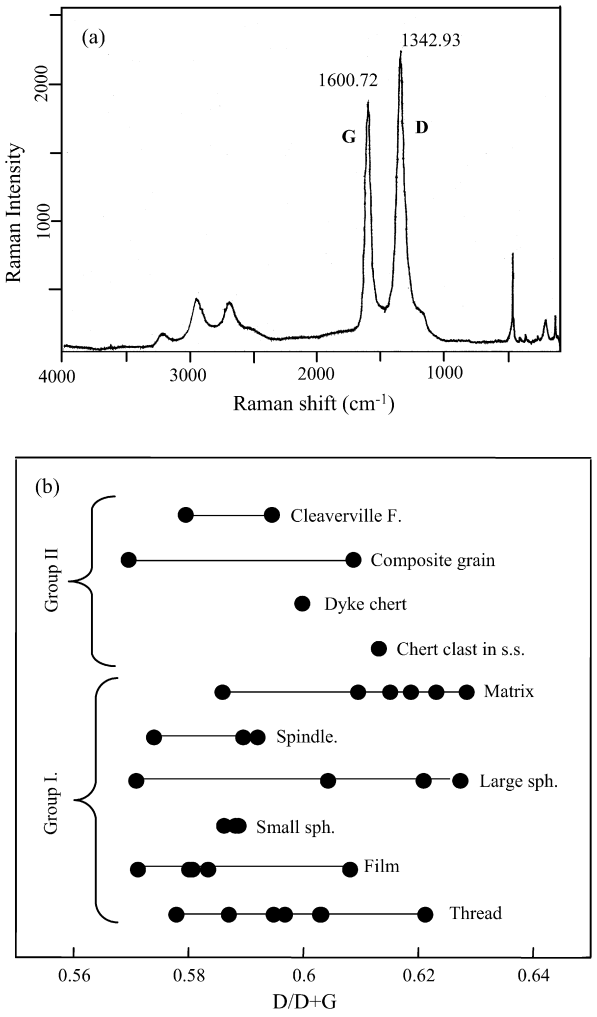

Fig. 8. (a) Representative Raman spectrum of carbonaceous microstructures. See text for interpretaion of D and G. (b) D/(D + G) ratios for representative morphological types of carbonaceous microstructures and carbonaceous matter of other occurrences. Groups I and II show data from the stratiform black chert containing microstructures and other lithologies, respectively. Matrix in Group I shows finely disseminated carbonaceous particles. Group II includes carbonaceous particles in laminated black chert in the Cleaverville Formation, composite grain in CE1 at Section 2 (Fig. 6a), composite grain in dyke chert at Section 3 (Fig. 6d), and black chert clast in sandstone at Section 1. These data were acquired on a Nicolet Almega XR under conventional analytical conditions at Nagoya University.

7. Bulk geochemistry

7.1. Major elements

The black chert is composed mostly of silica (>90%), with trace amounts of Al_2O_3, TiO_2, and Fe_2O_3* (total iron as Fe_2O_3) (Table 1). Total carbon concentration of the black cherts ranges from 0.03 to 0.12 wt.%, and sulfur concentration ranges from 0.003 to 0.21 wt.%. In general, the black cherts from Mount Goldsworthy contain higher C_{total} and S_{total} than those from Mount Grant.

7.2. Elemental compositions of kerogen (acid residues) and carbon isotopes

Elemental compositions and $\delta^{13}C$ values of kerogen obtained by HF-HCl digestion are shown in Table 2. The totals of elemental compositions are less than 100%, a result of the impurity of acid residues such as acid resistant sulfide. H/C atomic values in these acid residues range from 0.12 to 0.24, corresponding to a low metamorphic-grade (greenschist facies) (Hayes et al., 1983). $\delta^{13}C$ values (−31.9 to −35.4 per mil) are within the range of previously reported isotopic values for kerogen from early to middle Archaean cherts in the Pilbara Craton and in South Africa (e.g., Hayes et al., 1983; Schopf, 1993; Lindsay et al., 2005; Walsh, 1992; Ueno et al., 2001, 2004).

8. Morphology of carbonaceous microstructures

Four major morphological types of carbonaceous microstructures have been identified: (1) thread-like microstructures (Fig. 9a–f), (2) film-like microstructures (Fig. 10a–j), (3) spheroidal structures (Fig. 11a–n), and (4) lenticular to spindle-like microstructures (Figs. 12a–o and 13a–f). Each type includes several subtypes. All four types are abundant in massive black chert. Type (1) is present in both massive and some botryoidal chert, whereas types (2)–(4) are restricted to massive chert. Other morphological types have been identified, although only selected examples are referred to in this paper. Mounts Goldsworthy and Grant have many morphological types in common. Major morphological types and selected minor morphologies are described below and statistical parameters and associations between different types (Figs. 14a–c, 15a–c, 16) are noted.

Table 1
Major element compositions of black cherts

	Mt. Goldsworthy			Mt. Grant	
	GWM11A	GWM11A′-1	GWM11A′-2	ORW4B-1	ORW4B-2
SiO_2	>97	>97	>97	>97	>97
TiO_2	0.005	0.004	0.007	0.006	0.008
Al_2O_3	0.12	0.16	0.15	0.07	0.07
Fe_2O_3*	0.28	0.74	0.75	0.01	0.01
MnO	<0.01	<0.01	<0.01	<0.01	<0.01
MgO	0.02	0.02	0.02	n.d.	0.00
CaO	0.03	0.03	0.03	0.03	0.02
Na_2O	0.00	0.30	0.48	n.d.	0.06
K_2O	0.03	0.04	0.05	0.01	0.02
P_2O_5	0.004	0.003	0.011	0.006	0.003
H_{total}	0.008	0.011	0.012	0.005	0.005
C_{total}	0.123	0.074	0.057	0.027	0.028
S_{total}	0.108	0.205	0.070	0.004	0.003

Note. Total Fe as Fe_2O_3*.

8.1. Thread-like microstructures

Although some thread-like microstructures are present in the massive black chert, they occur mostly within the colloform-textured portions of cavity-fills and veins (Figs. 6c and 9a–f and for supplementary information, Supplementary Fig. I), as well as in evaporites replaced by black chert, again in colloform textured areas. In the massive chert lithology, thread-like microstructures are locally, restricted to the translucent, fenestra-like portions (Fig. 9c). In all cases, the threads are in a microcrystalline quartz matrix and their morphology is independent of both the quartz-matrix grain boundaries and the colloform lamination.

Thread-like microstructures are apparently solid throughout their length (Fig. 9a–c, e, f). The diameter of a single specimen is mostly uniform and is less than 1 μm. Two sub-types can be distinguished; one is relatively thick and has a granular or fuzzy surface (Fig. 9b and c), whereas the other is narrower and has a smooth surface (Fig. 9e and f). Length varies widely from a few tens of microns to several hundred microns. Long filaments are often highly twisted and entangled (Fig. 9b); some specimens may be branched.

8.2. Film-like microstructures

Film-like microstructures occur within massive chert (Fig. 10a–j, Supplementary Fig. II). Under high magnification (1000×), many of these microstructures have a granular appearance (Fig. 10a, b, f, h, j), whereas others, slightly better preserved, have a more hyaline appearance (Fig. 10c). Many of the film-like microstructures consist of an amorphous single sheet that has been folded (Fig. 10a, c, g–i), crumpled (Fig. 10b, d–f, i, j) and twisted (Fig. 10a, c, e, f, h, i). Total length and width cannot always be determined because of folding, but sizes range from about 50 to >500 μm. Folds are narrow and appear as dark linear features on photographs of the film surface, but are three-dimensional structures when viewed under the microscope (Fig. 10b, c, f, i). More complicated microstructures, such as that

Table 2
Elemental (wt.%) and isotopic compositions (per mil) of acid (HF-HC1) residues

	Mt. Goldsworthy			Mt. Grant
	GWM11A	GWM11A′-1	GWM11A′-2	ORW4B-1/2
N	0.04	0.03	0.01	0.09
C	34.06	17.44	26.86	65.28
H	0.46	0.36	0.45	0.66
S	26.06	41.12	30.74	3.34
H/C_{atm}	0.16	0.24	0.20	0.12
$\delta^{13}C$	−32.80	−35.40	−34.70	−31.90

Note. ORW4B-1/2 shows composite sample.

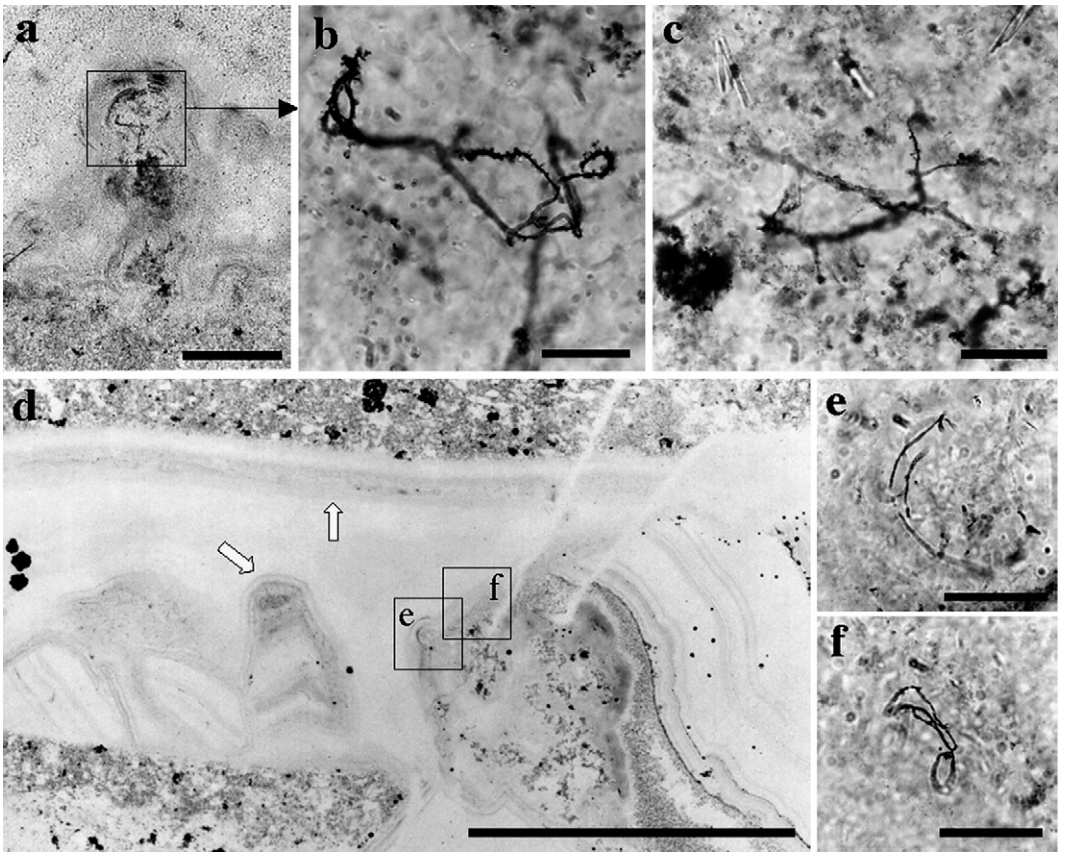

Fig. 9. Photomicrographs of thread-like microstructures. Scale bar: 200 μm (a); 20 μm (b, c, e, f); 1 mm (d). All specimens are from Mount Grant. See Supplementary Fig. I for Mount Goldsworthy specimens. (a) Colloform texture in white to translucent chert, in which the filamentous structure is enclosed. Slide ORW4B-8, Position L-K64/2. (b) Magnification of (a). Entangled thread-like filament with attached fine opaque particles. (c) Entangled filaments in a fenestra-like structure in carbonaceous massive chert. Slide NORW1X-4, Position L-O58/3. (d) Vein composed of microcrystalline quartz. Note that chert fragments and the vein wall are coated with carbonaceous laminae (colloform; the white arrows). Slide NORW1X-3, Position L-U45. (e) and (f) Magnification of (d). Very fine filamentous structures in carbonaceous laminae in vein.

shown in Fig. 10d, appear to be intensely crumpled film.

The microstructures have completely random orientations that are not controlled by crystal or chert-spherulite boundaries, or by any evidence of veining. They are embedded in the cloudy chert matrix (Fig. 10g), but there are sometimes patches of clearer chert in their immediate vicinity (Fig. 10e, g–i). Many sheets are tangential to the vertical and changes in orientation can be traced through the thickness of the thin section, indicating that they are not resting on bedding planes or related to any later deformational overprint. The actual morphologies of film-like microstructures are completely independent of the quartz-matrix grain boundaries. Their distribution is not related in any way to the colloform-textured and/or botryoidal areas. Surface texture varies from very smooth to granular, and some specimens are strongly folded, often unidirectionally (Fig. 10b and f). Where films are highly granular and wrinkled, they tend to be thicker than 5 μm, whereas smoother films tend to be less than 1 μm thick. Two types of film edge can be identified; one is irregular and notched (Fig. 10a and b) whereas the other is smooth and apparently thickened or rolled (Fig. 10a, c–f). This is not a consistent feature and only some edges have been affected.

In addition to the dominant single-layered films, some sheets appear multilayered (Fig. 10g). They consist of identical material to the single sheets. Some of them can be interpreted as large sheets that have been overfolded or rolled and that are viewed laterally because they lie at right angles to the plane of the thin section, rather than parallel to the viewing plane, as is the case with the single sheets. It is often possible to trace the layers tangentially through the thickness of the slide, indicating that they are indeed sheet-like rather than tubular or cylindrical. Individual sheets are gently wavy and partially granular, and

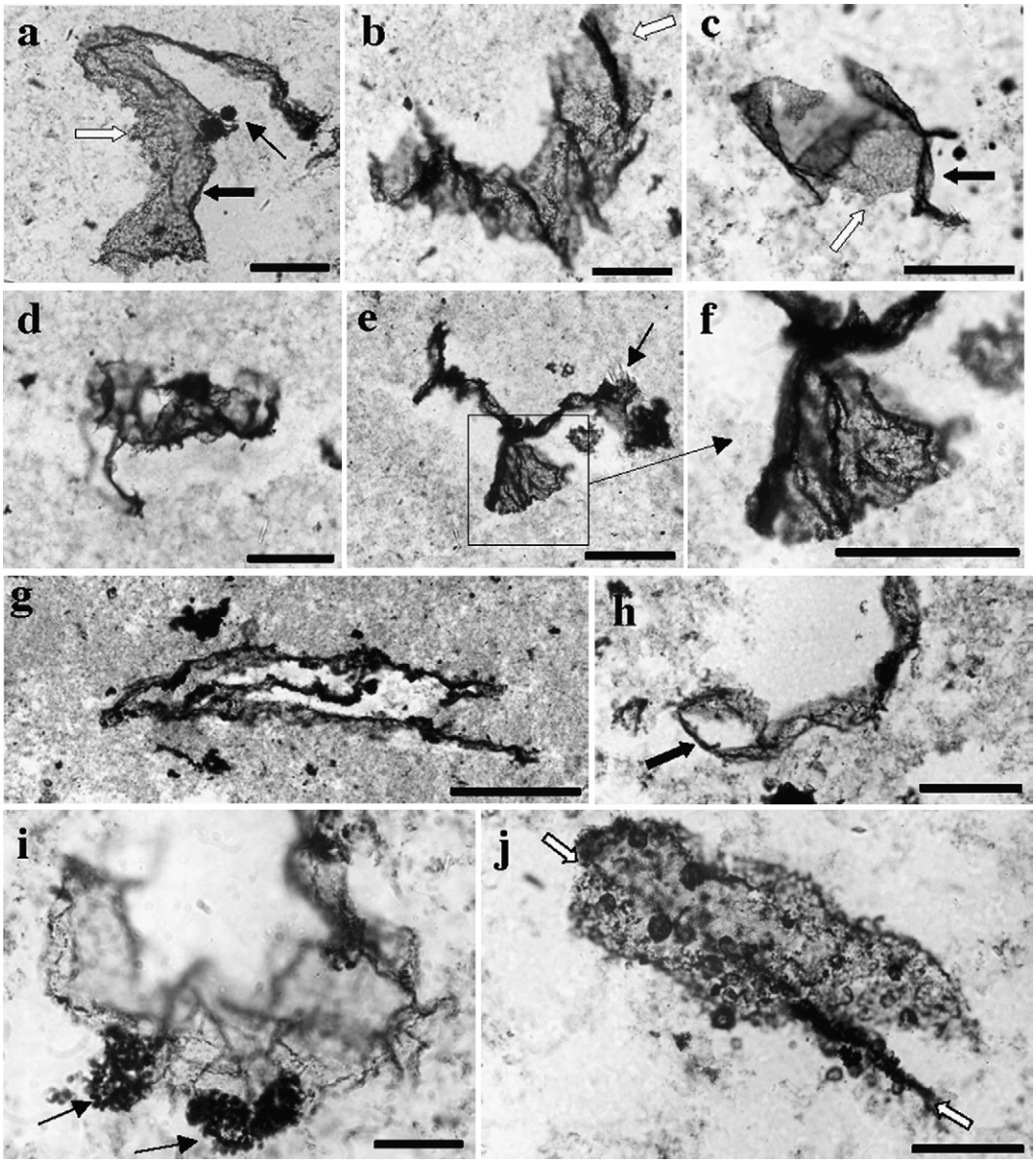

Fig. 10. Photomicrographs of film-like microstructures. Scale bar: 50 μm (a–f, h, j); 200 μm (g); 20 μm (i). All specimens are from Mount Grant. See Supplementary Fig. II for Mount Goldsworthy specimens. (a) Sharply angled film with clusters of fine opaque particles (the thin arrow). The white and solid arrows show notched and smooth rolled-up edges, respectively. Slide NORW1-05A, Position L-W50/3. (b) Gently angled (as seen in vertical view), unidirectionally wrinkled film with notched edge (the white arrow). Slide ORW4B-8, Position L-Q55/1. (c) Sharply kinked film with broad folds and both smooth rolled-up edge (the solid arrow) and notched edge (the white arrow). The surface of this specimen is more hyaline than other specimens illustrated here. The grainy texture is similar to that seen in degraded organic matter in younger rocks. Slide NORW1X-1′, Position L-Q47/4. (d) Loosely crumpled film with multidirectional wrinkles. Slide ORW4B-1, Position L-Q60/1. (e) Highly wrinkled branched film with twisted segment. The arrow shows cluster of prismatic crystals growing on the film. Slide ORW4B-1, Position L-U49/3. (f) Magnification of part of (e) showing rolled left edge and sub-parallel wrinkles. (g) Huge triple layered film, probably a lateral view of an overfolded sheet. Slide ORW4B-8, Position L-T53. (h) Single film, showing several twists and with a lenticular hollow structure at bottom left that is probably an overfold. Slide NORW1W-1, Position L-W64/1. (i) Delicate thin film showing crumpling and multidirectional wrinkling, with two clusters composed of opaque particles (thin arrows). Slide NORW1-05B, Position L-G54. (j) Film with rolled up edge, narrow mid-line fold (white arrows) and grainy surface with irregularly spaced semi-hollow small spheres. Slide NORW1Y-1, L-H49/3.

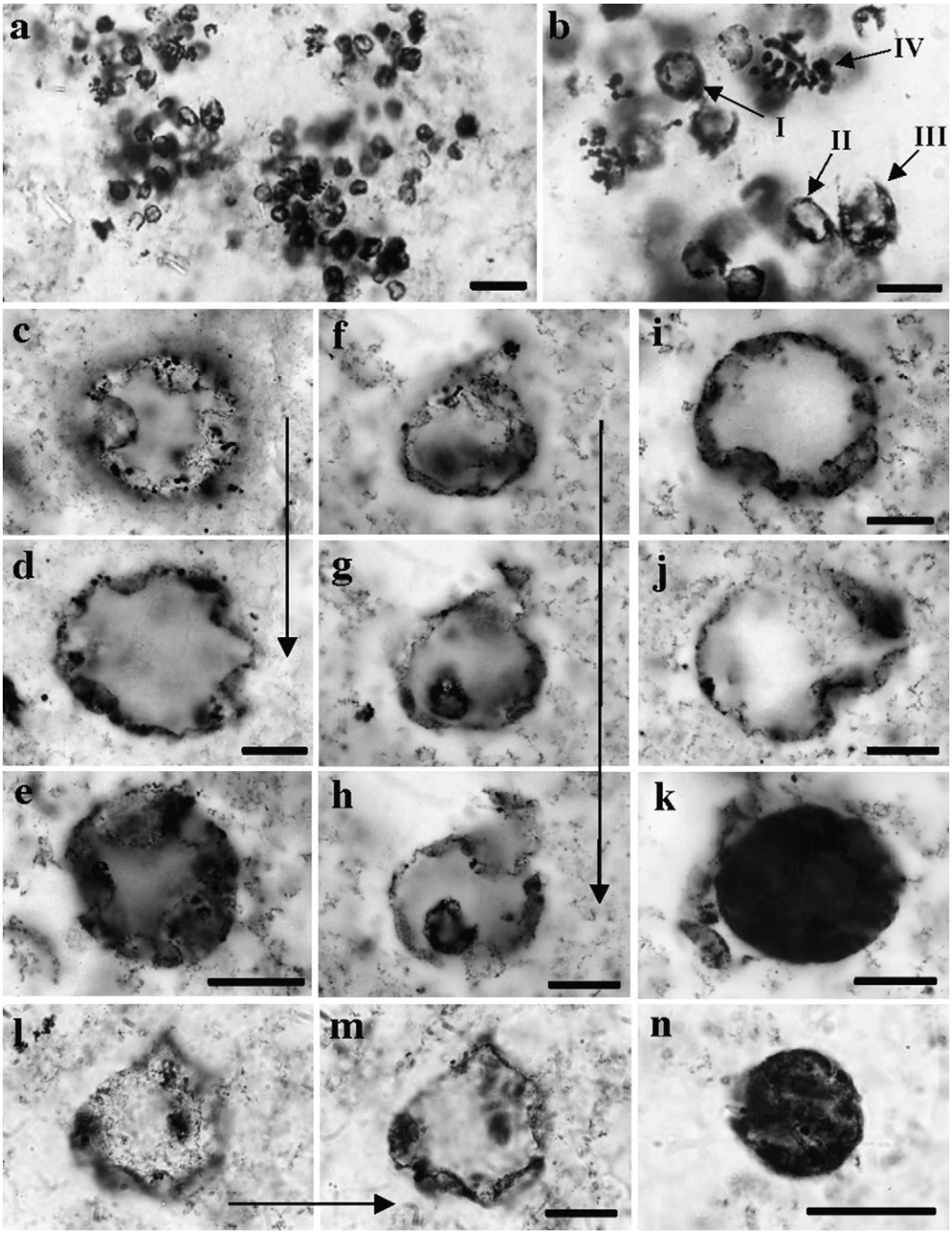

Fig. 11. Photomicrographs of spheroidal microstructures. Scale bar: 20 μm (a, c–n); 10 μm (b). (a), (b) and (l–n) from Mount Grant and others from Mount Goldsworthy. Also see Supplementary Fig. III. (a) Colony-like aggregation of small spheroidal microstructures. Slide NORW1, Position L-J50/2. (b) Magnification of (a). I, Nearly completely hollow sphere; II, distorted sphere; III, ruptured sphere; IV, cluster of opaque particles. (c) and (d) Polar and equatorial views of a large hollow spheroidal microstructures. Arrow shows the deepening focal depths. Slide GWM11A-sub2, Position L-R35. (e) Hollow spheroidal microstructures. Slide GWM11A-sub1, Position L-S46/4. (f–h) Views of hollow spheroidal microstructures with possible inner spheroidal object. The arrow shows the deepening focal depths. Slide NGWM1X, Position R-N40/1. (i) Slightly distorted hollow spheroidal microstructures with partially wrinkled wall. Slide NGWM3, Position R-L37/3. (j) Broken? spheroidal microstructure. Slide NGWM1X, Position R-F40/1. (k) Non-hollow spheroidal microstructure. Slide GWM11A-EX1, Position L-E38/3. (l and m) Distorted spheroid. Slide NORW1X-1', Position L-O59. (n) Semi-hollow spheroid with partly broken left margin. Slide GFWE3-1, Position L-O61.

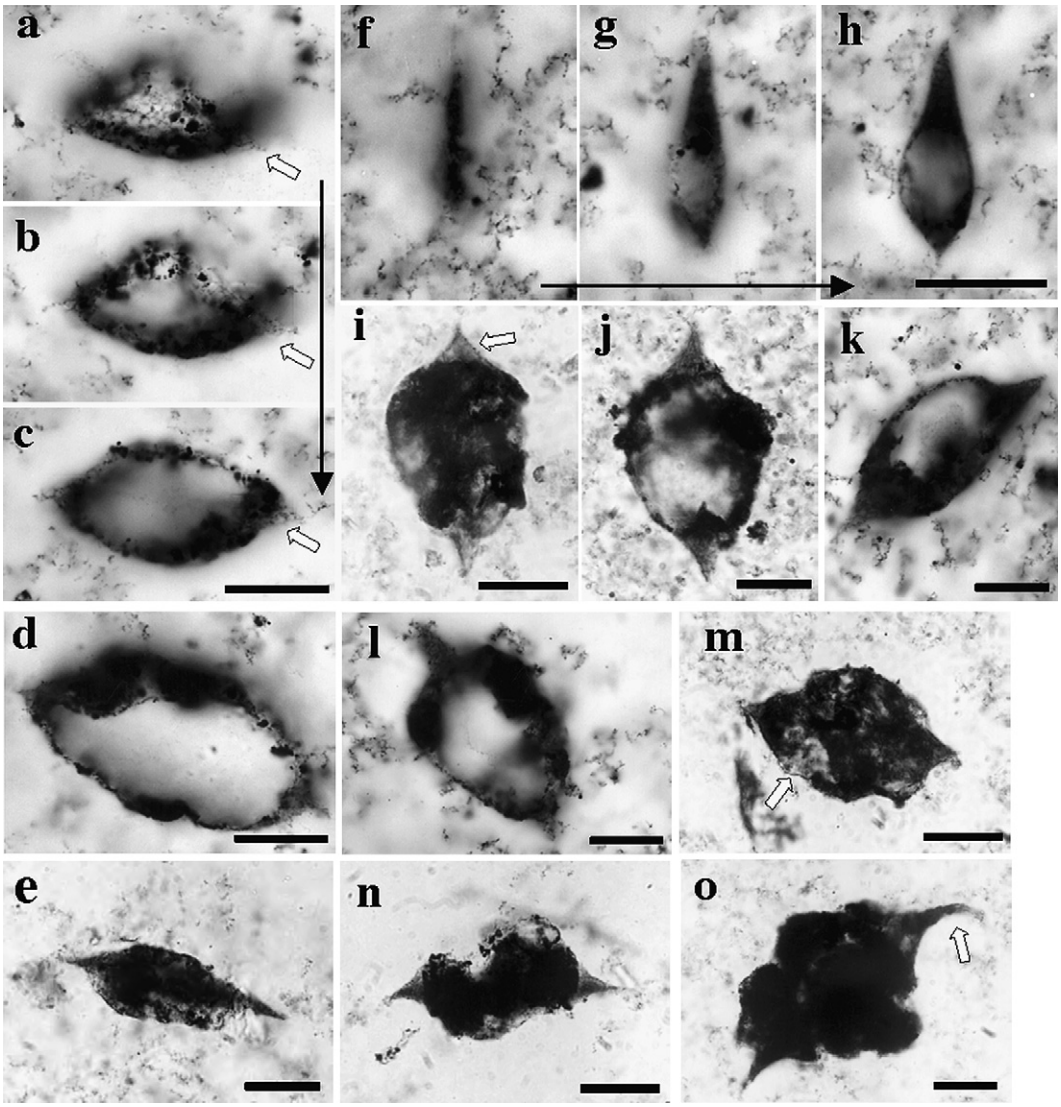

Fig. 12. Photomicrographs of spindle-like microstructures. Scale bar: 20 μm. (a–d), (f–h) and (j–l) from Mount Goldsworthy, others from Mount Grant. (a–c) Views of symmetric type at different focal depths from shallow to deeper (solid thin arrow). The white thick arrow indicates the flange-like appendage. Slide GWM11A-sub2, Position L-B36/2. (d) Hollow symmetric type. Slide NGWM3-sub1, Position R-R37/3. (e) Semi-hollow asymmetric type. Slide NORW1Y-2, Position L-R54. (f–h) Views of asymmetric type III (Fig. 15a) at different focal depths from shallow to deeper (solid thin arrow). Note that the long axis of this specimen is perpendicular to the local lamina of the lower half of Fig. 5e. Slide GWM11A-EX1, Position L-U45/2. (i) Semi-hollow asymmetric spindle-like microstructure. The membrane-like wall (white arrow) of the spherical body suggests that the flange is separate from the central body and that the flange is solid. Slide NORW1Y-3, Position L-M55/2. (j) and (k) Hollow asymmetric type I and III, respectively, with relatively thick wall. Wall-thickness is not uniform in (k) but thickens in the vicinity of the flange. Slide GWM11A-EX2, Position L-P37/3 for (j) and Slide GWM11A-7. Position L-T40 for (k). (l) Hollow asymmetric type I with 'geometric-shaped void' that is result of an angular hole in the proximal wall. Slide GWM11A-7, Position L-Z39/3 (Outside England Finder Grid). (m) Semi-hollow asymmetric type I with possible hexagonal authigenic mineral grain (arrowed). Slide NORW1, Position L-C59. (n) Broken? semi-hollow type. Slide NORW1-05B, Position L-P61/3. (o) Semi-hollow type with curved appendage (arrowed). Slide NORW1, L-N44/1.

like single-sheet films have either notched or thickened edges.

Though not common, film-like microstructures occasionally show apparent lens-like or blister-like structures (Fig. 10h). These appear to be folds that have remained uncompressed, suggesting that the material was floating in a colloid and that crystallization occurred rapidly and pervasively because it did not flatten the structures. Clusters of small, carbonaceous grains, much larger than the granules on the film or the finely disseminated particles in the chert matrix, are sometimes present on the surface of film (Fig. 10i). Some films have randomly dis-

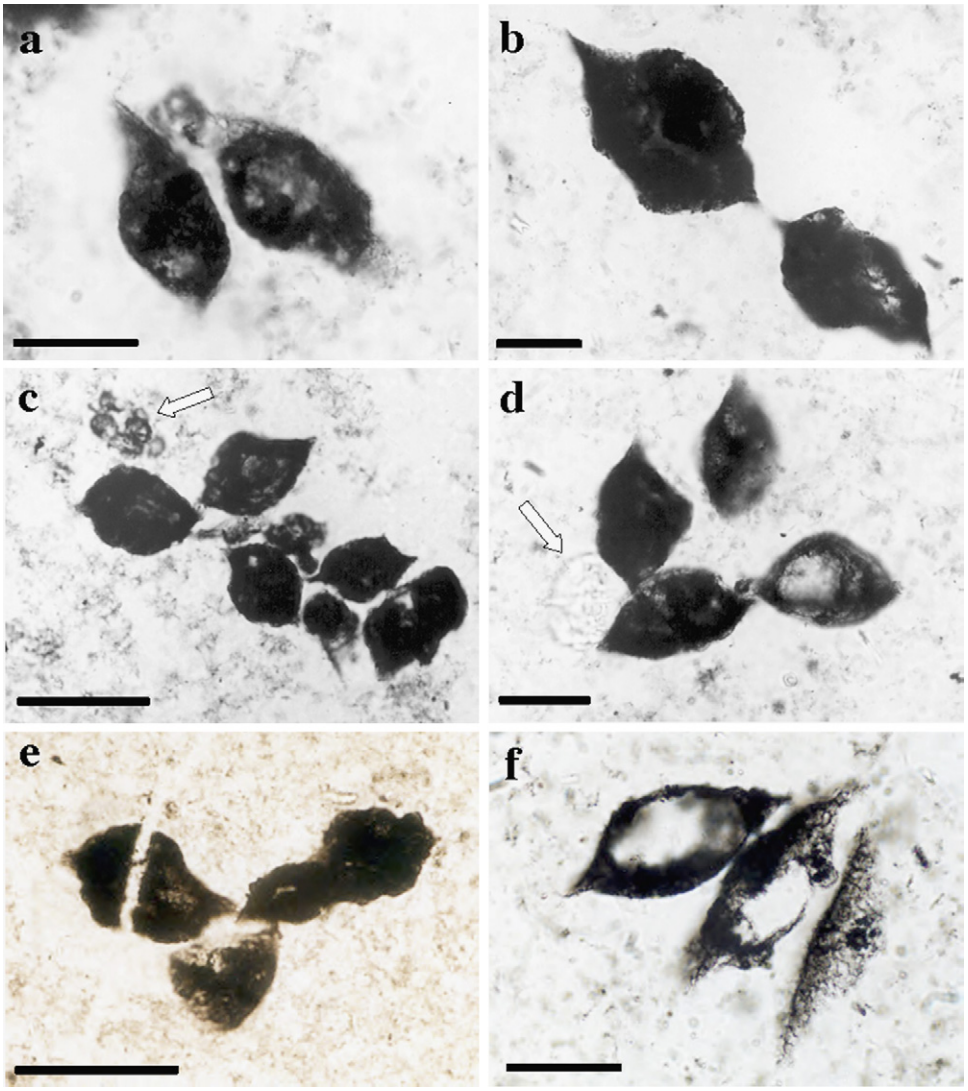

Fig. 13. Pairs and colony-like aggregations of spindle-like microstructures. Scale bar: 50 μm (c and e); 20 μm (a, b, d, f). All from Mount Grant. (a) and (b) Obliquely positioned and aligned pair structures, respectively. Slide NORW1, Position L-J44/4 for (a), Slide NORW1-05B, Position L-X61/4 for (b). (c) and (d) Colony-like aggregation composed of semi-hollow spindle-like microstructures. The arrow in (c) shows cluster of hollow spheres. The arrow in (d) shows a translucent crystal grain. Slide NORW1-05B, Position L-R52/2 for (c), Slide NORW1, Position L-W67 for (d). (e) Colony-like cluster composed of three microstructures of different morphological types. Note that the left specimen is cut by a narrow quartz vein, and that the bottom one appears to be split in half with the infill of chert. Slide ORW4B-3, Position R-N45/3. (f) Fan-shaped arrangement of three lenticular microstructures. Note that the two specimens on the right are sectioned at different levels, whereas the one on the left is embedded in the thin section. Slide GFWE3-2, Position L-X41/3.

persed, sparse, hollow spheres distributed on the surface (Fig. 10j).

8.3. Spheroidal microstructures

8.3.1. General features and size-distribution

Numerous spheroidal (including spherical) structures are present (Fig. 11a–n and Supplementary Fig. III). They are mainly hollow (Fig. 11a–j, l, m) or, more rarely, nearly solid (Fig. 11k) or semi-hollow (Fig. 11n). Spheroidal microstructures show a wide range of diameter (2.5 to >80 μm). Three-dimensional microscopic examination shows a hollow centre, now infilled with spheroidal chert, surrounded by patchily continuous walls up to about 1 μm thick. There is nothing to suggest that the walls formed as mullion structures by the movement of particulate matter as a result of spherulite growth (Brasier et al., 2005).

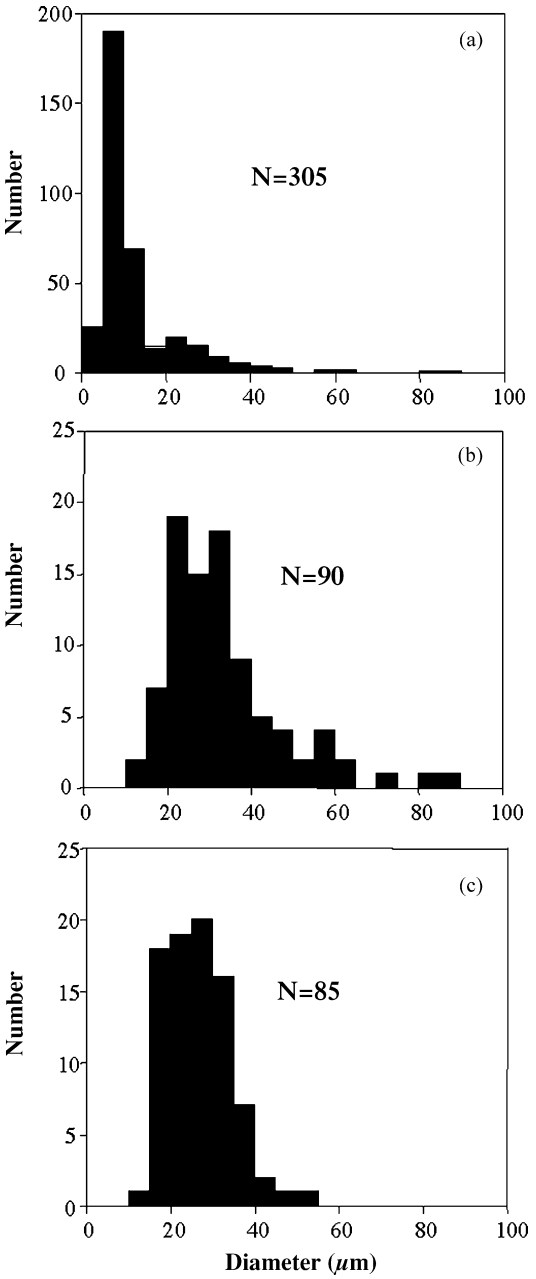

Fig. 14. Histograms of size (diameter) distribution of spheroidal microstructures. (a) All hollow spheroidal microstructures larger than 2 μm in diameter, including ambiguous ones. From slides GWM11A-sub2, -9, -EX1 and NGWM3. (b) Clearly identified thin-walled hollow spheroidal microstructures larger than 10 μm in diameter. From slides GWM11A (-1, -5, -7, -9, -sub1–5, and -EX1), NGWM (1X, 2-1, and 3), (c) Non-hollow spheroidal microstructures larger than 10 μm; from the same slides for (b).

Very small spheroidal objects less than 2.5 μm can be recognized but details are poorly preserved and their nature is difficult to distinguish so they are not considered further here. Size data for all hollow spheroidal objects larger than 2.5 μm (including some of the more ambiguous ones) shows a bimodal distribution with a dominant mode of 5–15 μm and a less clearly identifiable mode around 20–30 μm (Fig. 14a). The 20–30 μm mode is more obvious if only clearly identifiable hollow spheres larger than >10 μm are plotted (Fig. 14b). A similar distribution pattern is obtained when relatively large, semi-hollow, spheroidal microstructures are plotted (Fig. 14c). Because of the size-distribution trends shown in Fig. 14a–c, spheroidal microstructures are described below as being less than 15 μm in diameter, or larger than 15 μm in diameter (Fig. 11 and for supplementary information, Supplementary Fig. III).

8.3.2. Small (<15 μm) spheroidal microstructures

Small spheroidal microstructures occur solitarily and as aggregates (Fig. 11a and b). Pairs of spheres are also present but are not common. Spheroidal microstructures are occasionally associated either with films, as described earlier (Fig. 10j) or sometimes with other microstructures (see below). In many cases, the spheroidal microstructures appear to be hollow and have an uneven wall, similar to the wall architecture of some larger spheres as described below. Some spheroids are characterized by a highly granular wall surface, whereas in others, the walls have a patchy, mosaic-like pattern. Aggregates of spheroids commonly show a mixture of complete spheroids and distorted or broken shapes, as well as clusters of apparently opaque particles (Fig. 11b), although many of these are hollow when viewed in a different plane of focus.

8.3.3. Larger (>15 μm) spheroidal microstructures

Larger spheroidal microstructures are generally solitary. Aggregate microstructures are less common than in smaller spheroids; however, as described below, they are sometimes associated with other morphological types. Large, hollow spheroidal microstructures comprise about 50% of about 180 specimens recorded from the Mount Goldsworthy samples. About 90% of these ‘hollow’ specimens have interiors filled by spherulitic microcrystalline quartz displaying random extinction (Figs. 7c, 11d, e, i). The remaining hollow specimens (10%) have a single sphere-like object in their interior (Fig. 11g, Supplementary Fig. IIIf). In Mount Grant samples, hollow to semi-hollow spheroids appear to predominate. Numerous spheroids appear to have hollow, spheroidal microstructures aligned around the interior

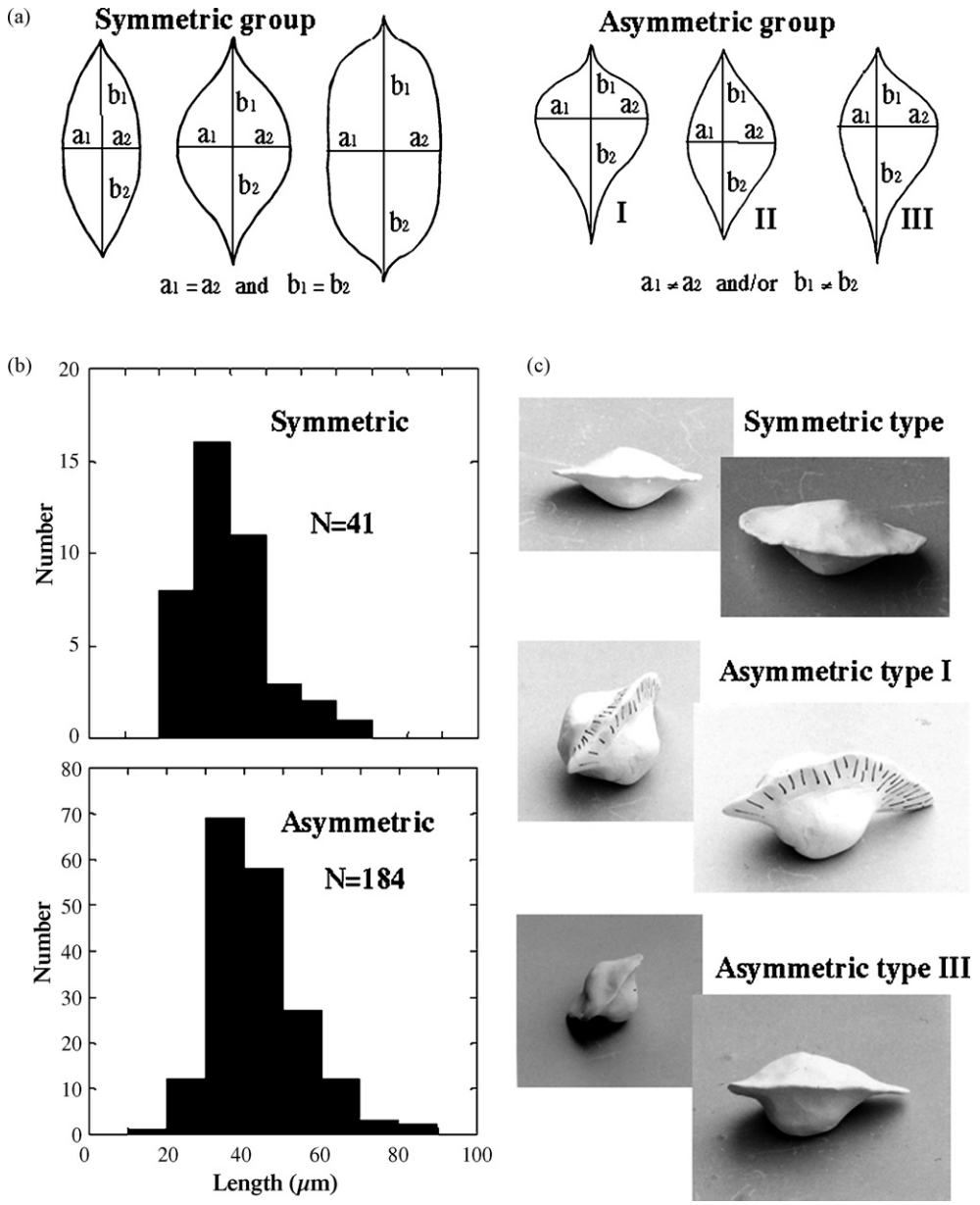

Fig. 15. Interpretations and measurements of spindle-like microstructures. (a) Hand-drawings of representative morphological types of spindle-like microstructures. The symmetric group is illustrated by a1 = a2 and b1 = b2, whereas the asymmetric group by a1 ≠ a2 and/or b1 ≠ b2. (b) Histograms for length along the long axes of spindle-like microstructures. Statistical data from slides GWM11A (-1, -5, -7, -9, -EX1, -sub1–5) and NGWM (1c, 2, 3, 1X, EX1). (c) Photographs of clay figures of spindle-like microstructures.

of the wall (Fig. 11c–j). Some of these are folds or blisters within the wall (Fig. 11c–f, h–j), but not all can be so readily explained, and some appear to be separate bodies within the sphere, sometimes attached to the wall (Fig. 11g), and sometimes apparently detached (Fig. 11g and h). Walls can be massive and continuous (Fig. 11d, f, g–i), at least in patches, but in thinner areas, as in film-like microstructures, the walls consist of a sheet with very fine granules or of fine carbonaceous particles. The wall is even or wavy to folded (Fig. 11d and i). Its thickness is generally less than 1 μm, although this is not clear in highly folded specimens. As exemplified by Fig. 11h–j, some hollow specimens have broken or distorted shapes.

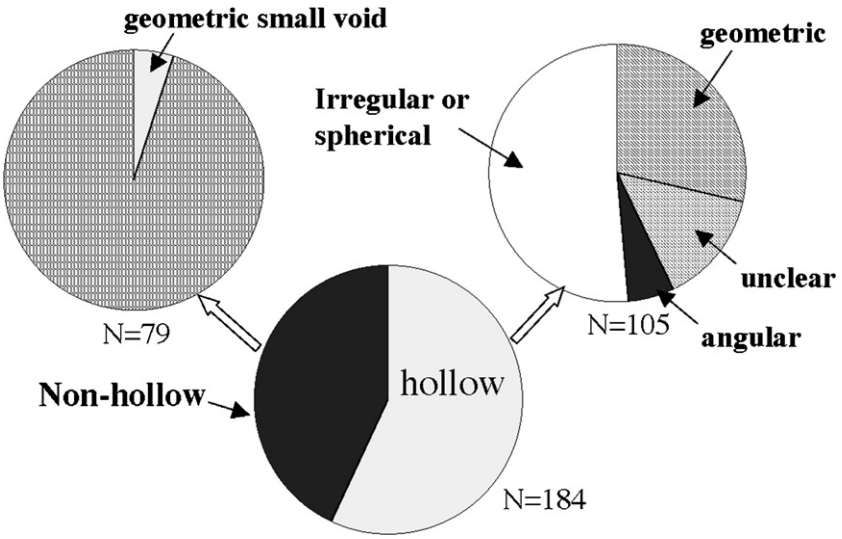

Fig. 16. Pie diagrams for internal textures of asymmetric spindle microstructures. Data sources are the same as for Fig. 15.

'Non-hollow' spheroidal structures are better described as semi-hollow rather than solid because they are characterized by various internal textures ranging from nearly homogeneous (Fig. 11k and n) to heterogeneous with irregularly shaped voids. Completely solid and massive specimens, like opaque mineral grains, are probably absent. Although the wall texture is rarely clear, some specimens have a very thick (>5 μm) wall or may have a wall that is strongly folded into the interior of the sphere.

8.4. Lenticular to spindle-like microstructures

The majority of microstructures other than the three types described above are lens-shaped, spindle-shaped or spheroidal with a spear-like appendage at either end when viewed at right angles to the equatorial plane (Figs. 12 and 13). All are grouped here as spindle-like microstructures and the following descriptions of their complex morphology are based on three-dimensional interpretation using an optical microscope.

Three-dimensional forms give rise to characteristic two-dimensional appearances in equatorial view, and the microstructures are either symmetrical (Figs. 12a–d, m–o and 15a) or asymmetrical (Figs. 12e–l and 15a). Out of 312 spindle-like microstructures from Mount Goldsworthy, 41 specimens are symmetrical and 184 are asymmetrical. Some specimens are difficult to classify because they have an equivocal shape. All specimens show a similar size distribution irrespective of morphological type (Fig. 15b). The lenticular body ranges mostly from 20 to 40 μm in length and 15–35 μm in width. Well-preserved appendages range from 2 to 10 μm in length. In the following, we describe representative specimens of the above-defined morphological groups, including their internal structure and wall architecture (Figs. 12a–o, 13a–f, 15b, c, 16 and for supplementary information, Supplementary Fig. IV).

8.4.1. Symmetrical spindles

In two-dimensional equatorial view, well-preserved symmetrical spindles (Fig. 15a) consist of a simple, hollow, lenticular body surrounded by a wall of uniform thickness of less than 5 μm, and with a solid-looking appendage at each end (Fig. 12a–d). The lenticular body is filled with microcrystalline quartz displaying random extinction, and commonly consisting of particle-bound spherulites identical in shape and size to those seen in the matrix and in spheroidal microstructures (Fig. 12c). In three-dimensional reconstruction, the appendages can be traced as a continuous structure around the equator, and is formed by an expansion of the wall into a solid, tapering structure that forms a flange, or girdle (equivalent to a zona or cingulum in palynological terminology), which completely encircles the central lensoid body. In many symmetrical specimens, the flange is visible as a narrow dark line of fairly uniform width that appears to bisect the central body. However, when examined at different depths of focus, the flange is only present on the upper and lower surfaces (Figs. 12a–d, 13f). At mid-level focus, the proximal surface of the flange abuts the spheroidal body and partially wraps around it in the equatorial plane (Fig. 12c, d, n), but there is no corresponding structure through the centre of the lensoid body. The flange structure does not extend to the polar regions; the wall thins to about 5 μm about one third of the dis-

tance from the equator to the pole and the wall retains a constant thickness of 5 μm across the polar region. The flange is up to 20 μm wide and tapers to a narrow distal edge. Features are consistent in numerous specimens. Three-dimensional reconstructions are illustrated in Fig. 15c.

8.4.2. Asymmetrical spindles

Asymmetrical spindles (Fig. 15a) can either show asymmetry along only the short axis (Subtype I) (Fig. 12i, j, l), or only along the long axis (Subtype II) (Fig. 12e); a third group (Subtype III) (Fig. 12f–h, k) is asymmetrical along both the long and short axes. Subtype II is rare and difficult to distinguish from the symmetric group.

In equatorial view, a flange, similar to that seen in symmetrical spindles, is present, and often appears as a linear shadow across the hollow lensoid body that becomes more clearly defined in higher or lower planes of focus (Fig. 12f–h). The visibility of the flange depends on the focal depth (Supplementary Fig. IVb–d). Flanges show some variability in size and style (Fig. 15c), although these variations result at least partially from differing orientations, rather than differing morphologies. Among the 184 asymmetric structures examined from Mount Goldsworthy, ca. 60% of the specimens have a hollow body filled with microcrystalline quartz, and the shape of the hollow central body varies from spheroidal to irregular. About 30% of the remaining hollow specimens appear to have a somewhat geometric interior, but in general these are hollow structures in which the upper or lower wall has been partially removed, so that the interior is viewed through the broken edges of the wall (Figs. 12l, 16; Supplementary Fig. IVb, f, g, i, j).

8.4.3. Other spindle-like morphologies

In addition to the fairly regularly shaped spindles described above, about 30% of specimens have an equivocal morphology that cannot be classified into any particular group. This may partly be due to their orientation, or to taphonomic factors, such as the disruption or distortion of the original shape; for example, the body may be partially torn or fragmented (Fig. 12n), or the appendage may be bent (Fig. 12o).

Spindle-like microstructures sometimes occur in pairs or in colony-like aggregations (Fig. 13a–f, Supplementary Fig. V). Paired microstructures are generally the same size and oblique to each other (Fig. 13a), although aligned pairs are also present (Fig. 13b). Most colony-like aggregates consist of tight to loose clusters of less than 10 relatively large (>20 μm) microstructures (Fig. 13c–f). Aggregates may contain more than one morphological type such as large spheroidal microstructures or indistinct irregular shapes.

8.5. Other carbonaceous microstructure morphologies

Other microstructural morphologies are present (Fig. 17a–l), although in low abundance; most are elaborate but problematic and some microstructures occur in linked groups (Fig. 17a, j, k).

One key specimen is a peapod-like microstructure, composed of three aligned semi-hollow objects apparently enveloped by a thin film (Fig. 17a). The three inner objects are of different sizes, and their shape is poorly defined, although one of them appears to be lenticular. Associated with the peapod-like microstructure are three other loosely aggregated, asymmetrical lenticular structures, showing a similar size range to the peapod-like microstructure.

Fig. 17b shows another cluster of three objects apparently enveloped by a thin film of hazy material. Again the three objects are not identical, but vary from a slightly flattened sphere with a relatively sharp outline (lower right, arrowed) to a less defined clot-like object (top). Although tubular filamentous microstructures are rare in the samples of black chert studied here, one example has been found from Mount Grant (Fig. 17c–e). This microstructure is about 15 μm in diameter and has a small, semi-hollow sphere inside.

Fig. 17f–h shows two clusters of small spheres apparently attached to a ribbon-like film and differs from the associations between small spheroidal microstructures and film-like structures described above. The spheres are hollow and of uniform size (about 5 μm in diameter). A broken sphere-like microstructure is accompanied by semi-hollow spheres of varying diameters and sphericity (Fig. 17i). Two lenticular objects are attached to each other in a chain-like alignment with a possible third, broken lenticular object in the middle (Fig. 17j), and another group of small spindle-like microstructures appear to be connected by a film-like strand. These lenticular bodies are smaller and more elongate than other spindle types already described (Fig. 17k). A very large (up to >100 μm) spheroid with a semi-hollow body and a single protrusion is also present (Fig. 17l).

9. Discussion

The controversy over Archaean microfossils has stimulated development of more stringent approaches to microfossil analysis. For example, Brasier et al. (2004, 2005, 2006) suggested that all Archaean putative micro-

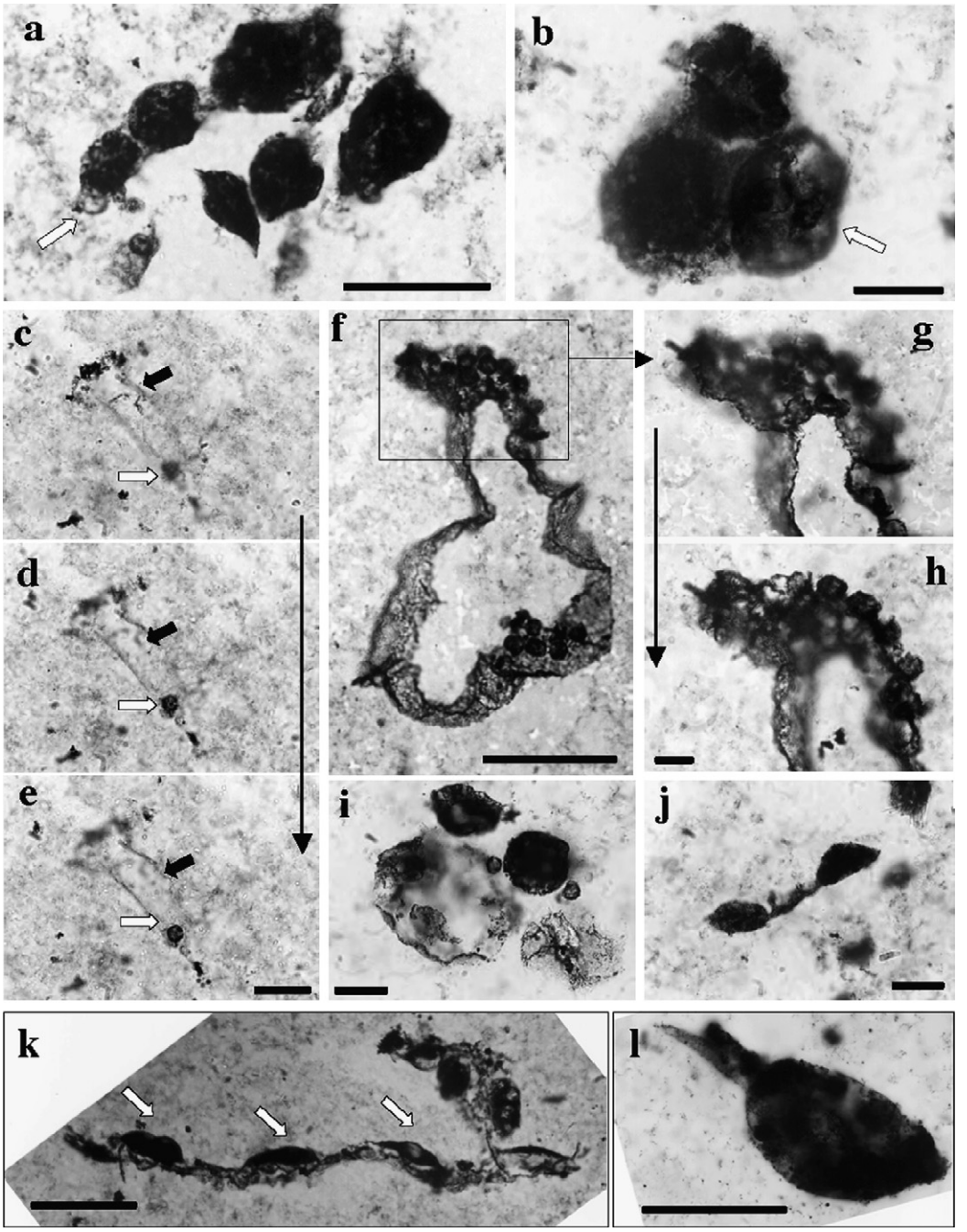

Fig. 17. Photomicrographs of carbonaceous microstructures of other morphological types. Scale bar: 50 μm (a, f, l); 20 μm (b, e, i, j, k); 10 μm (h). All from Mount Grant. (a) 'Peapod-like microstructure'. Note the size difference between spheroidal microstructures and the enclosing membrane. The white arrow shows a crystal grain attached to one side of this microstructure. Slide NORW1, Position L-D55. (b) Three objects including a possibly flattened sphere (the arrow) and associated hazy material. Slid NORW1, Position L-W61/2. (c–e) Hollow tubular microstructure with a single semi-hollow sphere (the white arrow) inside. The thin arrow shows increasing focal depths. The solid arrows indicate the portion of wall in focus. Slide ORW4B-7, Position L-M37/2. (f) Film-like microstructures with two clusters of small hollow spheroidal objects. Slide ORW4B-X1, Position L-W65. (g) and (h) Magnification of (f). Views of different focal depths. (i) Broken sphere-like structure and associated semi-hollow spheroids. Slide NORW1Y-3 (another chip from NORW1), Position L-T59/3. (j) Three lenticular microstructures (one of them is broken) organized in an attached chain-like alignment. Slide NORW1Y-2, Position L-U54/4. (k) Small spindle-like microstructures (the arrows) attached along a film-like objects. Slide NORW1-05B, Position R-E60/4. (l) Large spheroid with a single spear-like appendage. Slide NGWM1X, Position R-F40/1.

fossils need to be considered as non-biological until the "null hypothesis" (i.e., that the structures are non-biological) is refuted. However, we suggest that this latter approach cannot be constructively applied to Archaean palaeontology: Brasier et al. state that all 'other' (abiotic) possible means of formation must be excluded before a biological hypothesis can be accepted. If the words "all possible alternatives" implies inclusion of those that might be possible but have not yet been imagined, then it includes hypotheses that are untestable and are therefore not valid scientific hypotheses (also see Tice and Lowe, 2006). Therefore, there is no alternative but to test multiple working hypotheses by conventional palaeontological means. Previously published approaches, criteria and classification schemes remain valuable for interpreting Archaean microfossils.

A classification scheme proposed by Hofmann (1971, Fig. 1) designates structures as 'biologic, probably biologic, undecided, probably inorganic and inorganic'. Hofmann (1971) originally used the term 'problematica' for the middle three categories, but later (Hofmann, 1972) changed this to 'dubiofossil'. In the same publication, Hofmann proposed a set of criteria for recognizing a structure of biological origin. These criteria were applicable mainly to macrofossils; nevertheless, they provided a basis for many subsequent discussions and sets of criteria for recognizing biogenicity.

Schopf and Walter (1983) proposed four principle criteria, which can be summarized as: being of known provenance; being indigenous to the rock; being syngenetic; having attributes consistent with a biological origin. Since then, a number of other criteria have been put forward, including: (1) formation in an environment known to be suitable for life; (2) presence of degradational or taphonomic features; (3) the presence of biofabrics (based on the disposition of cells and organisms in their ambient biologic, environmental, and geologic context) (Hofmann, 2004). Some structures that do not display these characteristics may be biological, but the more of those characteristics that are present, the stronger the case for biogenesis. In the following section, we discuss the Farrel Quartzite microstructures in reference to the criteria.

9.1. Discussion of biogenicity criteria

Table 3 lists criteria for biogenicity based on previous literature (Schopf and Walter, 1983; Buick, 1990; Hofmann, 1994, 2004 and personal communication, 2006; Brasier et al., 2005; Westall and Folk, 2003). We have considered all the criteria suggested by these authors, but for reasons discussed above, do not find all of the proposed criteria acceptable. For example, we have problems applying the null hypothesis as stated by Brasier et al. (2005) to any fossils, not just putative Archaean ones. Some criteria proposed by Hofmann (1994), such as those relating to multicellularity, were intended for macrofossils, not microfossils, although the general principles apply. Brasier et al. (2005, Table 2) incorrectly quoted the colour index criterion proposed by Schopf and Walter (1983) and we revert to the correct version that states that the colour index of the microstructure should *not* be significantly different from the colour of the background material.

Another criterion included in Brasier et al. (2005) and based on Buick (1990) states that 'Filaments (or colonial unicells) should exhibit an orientation and distribution indicative of their role in the formation of stromatolitic laminae.' This criterion does not reflect the extensive records about the habit of microfossils recorded in the geological literature. Associations between stromatolites and preserved microfossils are extremely rare. Many examples of Proterozoic and Phanerozoic microfossils preserved in chert have nothing to do with stromatolite formation and microfossils are randomly oriented within the chert, and were probably originally suspended in colloidal silica. Some of the widely accepted 800 Ma Bitter Springs Formation microfossils (Schopf, 1968) would not meet the criterion because they are not necessarily associated with lamination within the chert.

Microfossils can be associated with non-stromatolitic benthic mat fabrics and other biofabrics, and where this occurs, it is a good indication of biogenicity. The criterion has been modified to reflect this possibility: 'Ideally, microstructures should resemble filaments or colonial unicells, and may exhibit an orientation and distribution indicative of their role in the formation of biofabrics such as stromatolitic laminae or other type of mat fabric' (Table 3, (14)).

Table 3 lists the criteria that are relevant to recognizing biogenicity and summarizes the results when applied to the Mount Goldsworthy and Mount Grant microstructures. For our study we have grouped the criteria into (1) geological context, (2) indigenousness and syngenicity, (3) biologically acceptable context, involving biologically acceptable occurrence, biologically acceptable morphology, and biologically acceptable processes, and (4) biologically acceptable chemistry, based in part on groupings suggested by Brasier et al. (2005).

9.1.1. Geological context

The microfossils are present in rocks of known provenance, and their context has been confirmed by replicate sampling. The host black chert is of a known prove-

Table 3
Criteria for biogenicity and application to Mt. Goldsworthy and Mt. Grant microstructures

Modified criteria based on previous studies	Application to microstructures in the present study	Threads	Films	Large spheres	Small spheres	Spindles
Geological context						
(1) Microstructures should occur in rocks of known provenance, confirmed by replicate sampling (1, 2)	Samples are from Mount Goldsworthy and Mount Grant in the East Pilbara Terrain. Replicate samples of those collected in 2001 were obtained on successive visits in 2003, 2004, 2005 and 2006	Y	Y	Y	Y	Y
(2) Microstructures should occur in host rocks of established age (1, 2, 3)	Host rocks occur in Archean siliciclastic sedimentary unit correlative to the Farrel Quartzite of the Gorge Creek Group, and are older than 2.9 Ga	Y	Y	Y	Y	Y
(3) Microstructures should occur in a sedimentary or low-grade metasedimentary host rock (1, 2, 3, 4)	The sedimentary origin of host rocks is well demonstrated by sedimentary structures, relationship with overlying and underlying clastic layers, brecciation by overlying sandstone, presence of clastic laminae. The microfossiliferous stratiform black chert extends laterally >2 km along the strike. Low-grade metamorphism is demonstrated by Raman spectra and size of matrix microquartz (mostly <5 μm)	Y	Y	Y	Y	Y
(4) Microstructures should occur in rocks demonstrating geographic extent and geological plausibility (2,4)	Found at the same horizon at >5 separate localities. Geographical extent demonstrated by regional mapping	Y	Y	Y	Y	Y
(5) Potential biosignals should be referable to a well-defined history within the geological context at a wide range of scales from outcrop to thin section (2)	Microstructures were present at time of primary silicification (see text)	Y	Y	Y	Y	Y
Indigenousness and syngenicity						
(6) Microstructures should be demonstrably indigenous to the primary deposition of the enclosing rock (1, 2)	Microstructures (except for thread-like structures—see text) are present in standard thin sections, in the plane of the thin section, where they are restricted to primary chert clasts, the oldest component of the chert breccia. Some microstructures are oriented parallel to primary sedimentary laminae	N	Y	Y	Y	Y
(7) Microstructures should be demonstrably syngenetic with a primary phase of the enclosing rock and not in phases of post-depositional events such as replacement and displacement (1, 2)	Microstructures (except threads) are in a primary chert phase and occur in randomly extinguishing microcrystalline quartz (Brasier et al., 2005). They were present during the formation of the early diagenetic chert spherulites. They are not enclosed in any metastable mineral phase, nor in second generation void-filling minerals (e.g., botryoidal chalcedony), or radially extinguishing micro-quartz after fibrous chalcedony. None of the structures occur in planar, infilled-mineral veins, or are concentrated at mineral grain boundaries, or exhibit cross-cutting relationships in which they have disrupted primary features of the lithified rock fabric (Brasier et al., 2005). By contrast, some structures are cross-cut by later veins	N	Y	Y	Y	Y

Table 3 (*Continued*)

Modified criteria based on previous studies	Application to microstructures in the present study	Threads	Films	Large spheres	Small spheres	Spindles
(8) Microstructures should *not* exhibit a significantly different colour from that of the particulate finely laminated kerogenous component of the rock matrix (1, *not* 2)	This has been demonstrated by visual inspection and Raman spectra. They both exhibit a TAI of 5- (very dark brown to grey)	Y	Y	Y	Y	Y
(9) Microstructures should not be exogenous (for example, endolithic) (1, 5)	There is no evidence of contact between the microstructures and the rock surface. They show the same degree of thermal maturation as the finely disseminated carbonaceous material in the matrix and cannot be endoliths or any other microorganisms of recent origin because such structures would be pale yellow to straw in colour. In two examples they are aligned parallel to bedding	Y	Y	Y	Y	Y
Biological context (biofabric of Hofmann, 2004)						
(10) Microstructures should occur in a geological context plausible for life (1, 2, 4)	Palaeoenvironmental data are consistent habitats for life. Association with evaporites indicates a shallow water environment	Y	Y	Y	Y	Y
(11) Microstructures should be relatively abundant and occur in a multi-component biogenic assemblage (morphological diversity) (1, 2, 4, 6)	Four major morphological types, each with several subtypes have been identified. More than 50 specimens are present in most thin sections (3.2 cm × 2.4 cm)	Y	Y	Y	Y	Y
(12) Ideally, microstructures should fit within a well-established evolutionary context (2)	As far as the evolutionary framework is known, they fit within the context	Y	Y	Y	Y	?
(13) Ideally, microstructures should occur in associations indicating colonies, communities and mats (4). Not all microfossils will meet this criterion	Some microstructures, especially some spindle structures, show evidence of association and film structures may be degraded mats (see text)	Y	Y	Y	Y	Y
(14) Ideally, microstructures should resemble filaments or colonial unicells, and may exhibit an orientation and distribution indicative of their role in the formation of biofabrics such as stromatolitic laminae or other type of mat fabric (3). Only rarely will microfossils meet this criterion	Not observed in these samples (resemble filaments and unicells, but no evidence of orientation and no reason why this should occur in non-laminated chert)	N	N	N	N	N
(15) Ideally, microstructures should occur in the form of cell aggregates, cell envelopes, microborings, or waste products, within a restricted morphospace (2). Not all microfossils will meet the first two criterion and the remainder will be met only in exceptional circumstances	A few structures appear to have envelopes	N	N	N	Y	Y

Table 3 (*Continued*)

Modified criteria based on previous studies	Application to microstructures in the present study	Threads	Films	Large spheres	Small spheres	Spindles
(16) Microstructures should show evidence of taphonomic degradation (6)	Numerous examples of taphonomic degradation (such as folding, fracturing, rolling) are present	N	Y	Y	Y	Y
Morphological characteristics						
(17) Ideally, microstructural morphology should be comparable to that exhibited by modern microorganisms or well-documented fossils from younger successions (1,2, 4)	Difficult to determine because of simple morphology. However, spheres resemble well documented fossil morphologies (see text)	Y	Y	Y	Y	?
(18) Microstructures should be larger than the smallest extant free-living organisms (>0.01 μm^3) (3)	All microstructures identified in this study are larger than 5 μm	Y	Y	Y	Y	Y
(19) Microstructures, especially spheres, should be hollow and cellularly elaborate, and contain ultrastructures (2, 3, 4). Not all microfossils will meet this criterion	Threads and films are not hollow, but some show cellular elaboration. Most spheroidal and spindle-shaped microstructures are hollow. Ultrastructure not discernable in this study	N	Y	Y	Y	Y
Evidence of biological processes						
(20) Microstructures should be characterized by a range of (statistically demonstrable) variability (rather than uniformity), including life cycle variants, vital functions, cellular differentiation and degradation (1, 2, 4, 6). Not all microfossils will meet this criterion	Structures that could be interpreted as reproductive stages are present, but this is difficult to confirm at this stage (see text)	?	Y	Y	Y	Y
Biochemical context						
(21) Microstructures should be the primary source of palaeontological data from examination in petrographic thin section, but biogenic authenticity should be verified by the use of independent analytical techniques (1, 2)	This was the approach taken	Y	Y	Y	Y	Y
(22) Ideally, microstructures should be of carbonaceous composition (1, 2, 3, 4) or if mineralic, should be a result of biologically mediated mineral encrustation or a product of mineral emplacement (1). Not all microfossils will meet this criterion	All morphological types were tested by Raman spectra and found to consist of carbon. The structures are not mineralic so the second part of the criterion does not apply	Y	Y	Y	Y	Y

Table 3 (*Continued*)

Modified criteria based on previous studies	Application to microstructures in the present study	Threads	Films	Large spheres	Small spheres	Spindles
(23) Ideally, microstructures should show the presence of extracellular polymeric substances (EPS) and organominerals (2, 5). Not all microfossils will meet this criterion	Film-like structures may originally be EPS. Specific organominerals have not yet been identified. Not all organisms produce EPS, so this criterion is questionable	?	?	?	?	?
(24) Microstructures should be dissimilar from potentially coexisting abiologic organic bodies (e.g., proteinoid microspheres, carbonaceous 'organized elements', and products of organic synthesis (1, 2)	Microstructures do not resemble co-existing abiogenic structures	?	Y	Y	Y	Y
(25) Chemical biomarkers should include carbon isotopes or should be specific organic compounds (2)	Bulk carbon isotopes are not inconsistent with a biogenic origin	Y	Y	Y	Y	Y
Other criteria and concepts						
(26) The null-hypothesis (of an abiological origin for the morphology and processes) should be falsified (2)	See text discussion	?	?	?	?	?

(1) Schopf and Walter (1983), (2) Brasier et al. (2005), (3) Buick (1990), (4) Hofmann (1994), (5) Westall and Folk (2003), (6) Hofmann (2004).

nance that indicates an undisputed Archaean age. The rocks show a significant lateral extent and are of sedimentary origin. They are thought to have been deposited in a shallow environment in a continental margin setting. Metamorphic grade is lower than middle greenschist facies. The host black chert meets the criteria for 'geological context'.

9.1.2. *Indigenousness and syngenicity*

All microstructures are from standard petrographic thin sections cut from fresh rock surfaces obtained from stratigraphically and lithologically controlled sections. All microstructures, except for thread-like structures, occur only in primary chert clasts, the earliest phase of formation. Where the margins of clasts have been bleached, they show the same degree of alteration as the carbonaceous particles in the matrix. They cannot be endolithic microbes, because they show a similar degree of thermal maturity to carbonaceous particles and clots in the matrix. Indigenousness and syngenicity are thus demonstrated for spheroids, films, and spindles. The presence of the microstructures at an early stage of chert formation is indicated by the relationship to the spherulitic chert matrix and because the structures are cross cut by later veins (Figs. 7c1, 13e).

9.1.3. *Biologically acceptable context*

The microstructures, all of which are larger than 1 μm and up to 100 μm in length, are composed of diverse morphological types. Each morphological group (thread, film, spheroid, spindle) can be further subdivided. Many morphological groups contain multiple specimens. There are minor variations in shape, size and preservation. Such features are consistent with the range of morphological variation seen in biological specimens, and with post-mortem degradation and diagenetic alteration (taphonomy). Multiple specimens occasionally occur as aggregates (Fig. 13, Supplementary Fig. V) in which different combinations of morphological types are involved (for example in Fig. 17k where a film combines with small spindle shapes) and this occurrence could be interpreted as colonial or community-like occurrences. Continuous mat-like lamination has not been seen in the present samples, although film-like structures could be interpreted as fragmented and reworked mats. Structures that could be interpreted as possible cell-envelopes are found in a few specimens (Fig. 17a).

Microstructures have a range of morphology consistent with biogenic morphologies, particularly among prokaryotes, although the simple plan of structures such as spheroids, threads, and filaments limits direct com-

parison to modern microorganisms. The large size of the spindles is unusual for rocks of this age, and only a few prokaryotic organisms reach such large dimensions (e.g., Schulz and Jørgensen, 2001). The microstructures, particularly the large hollow spheres, resemble many fossils recorded from younger rocks. The variability observed in the dimensions of aggregations of small spheres, larger spheres, and spindles is consistent with size distributions observed in biological organisms and usually attributable to growth and morphological variation. Film-like microstructures may be the remains of extracellular polymeric substances (EPS) and the granular texture and small embedded spherical microstructures are similar to features found in many coccoid bacterial mats. Some groupings show features that could be interpreted as evidence of reproduction. However, studies are at too early a stage for comparisons with extant morphologies to be meaningful.

Spheres, spindles and films all show features consistent with degradation (taphonomy), such as surface folds, wrinkling, and fragmentation. For example, chert microfossils (particularly of *Myxococcoides grandis*) from the 1400 Ma Billyakh Group of the Anabar Uplift, northern Siberia contain similar internal bodies and invaginations of the wall to those illustrated here (Sergeev et al., 1995; Sergeev, 2006). Such features are regarded as taphonomic in origin in younger microfossils. The presence of taphonomic features is unlikely in abiogenic structures.

The morphological variations of the microstructures summarized above are not compatible with formations as biomorphs (García-Ruiz et al., 2002, 2003). Biomorphs, or probably more correctly abiomorphs (Hofmann, 2004), are morphologically diverse and complex crystal aggregates produced by barium-silicate solutions at ambient temperature and pressure in alkaline conditions (pH 8.5–11) (García-Ruiz et al., 2002, 2003). Theoretically, a specific microstructural morphology could be attributed to a specific abiomorph shape, but it would be difficult to produce an assemblage of different morphologies given that abiomorph formation is strictly controlled by physico-chemical conditions (e.g., Fig. 4c). Additionally none of the described biomorphs show the morphological complexity of the spindles or the presence of internal structures (Supplementary Figs. IVa and Vb).

9.1.4. Biologically acceptable chemistry

Microstructures reported here are carbonaceous, as confirmed by Raman analyses. Although individual values have not yet been determined, bulk isotopic values are significantly lower than those for abiogenic carbonaceous matter in chondrites and are within the range for biogenic values.

9.2. Interpretation of Farrel Quartzite microstructures

Application of criteria for biogenicity strongly supports an interpretation as biogenic. The criteria for recognizing biogenicity still require refinement. For example, the significance of some important features, such as morphological incompleteness (e.g., Fig. 11j), narrow size distributions (Figs. 14 and 15), and taphonomy have not been widely recognized. In the following sections, we attempt a comprehensive interpretation of each group of microstructures, using Hofmann's three categories of fossil (microfossil), dubiofossil (dubiomicrofossil), and pseudofossil (pseudomicrofossil). This terminology has proved valuable in previous interpretations of enigmatic structures, despite criticism of the terms by Brasier et al. (2005). The categories have long proved useful for discussions and provided a practical and realistic approach to a problem in which there is often no absolute solution, as opposed to taking a philosophical approach that requires the outcome to be unequivocal. Following Hofmann (1971, 1972), a (genuine) fossil is a structure of certain biological origin; a pseudofossil is a structure of undoubted non-biological origin (i.e., a structure produced by purely physical or chemical processes); a dubiofossil is a structure whose origin is uncertain. These categories can be further subdivided by the use of terms such as possible microfossil and probable microfossil.

9.2.1. Thread-like microstructures

These microstructures often cross cut the matrix of colloform laminae, indicating that they are not merely concentrations of organic particles at crystal boundaries. The twisted or entangled morphology of some specimens (Fig. 9b) implies that they were composed of flexible material, although ambient pyrite trails often show similar microstructure (Tyler and Barghoorn, 1963; Knoll and Barghoorn, 1974; Awramik et al., 1983; Grey, 1986). Their occurrence in cavity-fill secondary phases does not entirely exclude the possibility of biogenicity, as subsurface environments are now widely accepted as habitats for microbial life, especially for chemotrophic bacteria (e.g., Al-Hanbali et al., 2001; Buick, 1984; Ghiorse, 1997; Hofmann and Farmer, 2000; Walter, 1996).

Although solid filamentous microstructures have been reported from other Archaean rocks as part of hydrothermal vein systems and ore deposits showing colloform structure, as well as from normal sedimentary cherts (Awramik et al., 1983; Kiyokawa et al., 2006; Rasmussen, 2000; Ueno et al., 2001; Walsh, 1992; Walsh and Lowe, 1985), it is difficult to successfully

demonstrate their biogenicity because of their simple morphology, (e.g., Awramik et al., 1988; Buick, 1984, 1988). It is also difficult to claim a biogenic origin for thread-like microstructures observed in this study because their geological context is uncertain, and they must be regarded as dubiofossils.

9.2.2. Film-like microstructures

These microstructures are very variable in shape; they can be folded (sometimes into several layers), twisted, crumpled, and wrinkled (Fig. 10a–j). Edges are generally notched or torn, or appear thicker than other parts of the film, a feature consistent with the edges being rolled up (Fig. 10a, c, e, f). Taken as a whole, all these characteristics suggest that the film-like microstructures were once composed of flexible, tearable, and sometimes breakable matter. The variability and flexibility is incompatible with formation as a crystalline substance.

Some film-like microstructures have a smooth surface, composed of densely and homogeneously distributed, fine carbonaceous matter, whereas others have granular surfaces. The range of observed features are indicative of taphonomic degradation (Hofmann, 2004); some appear to be better preserved than others, and the pattern of degradation follows that seen in numerous fragments of organic mat-like material throughout geological time (Renaut et al., 1998; Westall et al., 2000). Film-like microstructures produced through abiogenic processes, such as fluid invasion of fractures, do not have complex features like rolled-up edges. Displacement of carbonaceous particles by the growth of botyroidal and spherulitic chalcedony (Brasier et al., 2005) does not explain the irregular wrinkled surface and uneven morphology.

These lines of evidence are consistent with a biogenic origin for most of the film-like microstructures and they are here classified as probable microfossils. Those associated with small spheroids or particle aggregates are most likely to be biogenic, probably originally as a biofilm or bacterial mat. A biofilm is a community of microorganisms composed of cells and mucous extracellular polymeric substances (EPS), which is usually attached to a surface (e.g., O'Toole et al., 2000). Carbonaceous laminations and mineralized film-like structures in Archaean chert from Barberton Mountain Land, South Africa and Pilbara Craton, Western Australia have been interpreted as biofilms (biomats) (Tice and Lowe, 2004; Westall et al., 2001; Westall et al., 2006), although film-building microbes were rarely identified. In the present study, the tiny hollow to semi-hollow spheres could be candidates for fossilized film-building microbes. Westall et al. (2001) noted that bubble-shaped or lenticular structures could be formed within a biofilm by metabolically produced gases. This process could explain some of the apparent, lenticular structure of some of the films, although most probably formed simply as fold structures (see Fig. 10h).

9.2.3. Small (<15 μm) spheroidal microstructures

Spheroidal microstructures have been reported from many Archaean carbonaceous cherts (e.g., Dunlop et al., 1978; Knoll and Barghoorn, 1977; Nagy and Nagy, 1969; Walsh, 1992). However, the biogenicity, especially of small ones, has not yet been demonstrated unequivocally (Schopf and Walter, 1983 and references therein). This is because such simple morphology can be produced by abiogenic processes (e.g., Herdiantia et al., 2000; Herzig et al., 1988; Oehler, 1976). As in many previously reported examples, detailed features of small spheroidal microstructures in this study cannot always be clearly demonstrated. Nevertheless, the following features suggest a biogenic origin for small spheroids that occur as colony-like aggregations or in a close association with film-like microstructures: (1) carbonaceous composition (2) hollowness, (3) narrow size distribution, (4) morphological variation suggestive of flexibility, (5) the presence of colony-like aggregations, and (6) morphological variability suggestive of taphonomy. They are here regarded as probable microfossils.

9.2.4. Large (>15 μm) spheroidal microstructures

As with the small spheroidal microstructures, the biogenicity of relatively large (>10 μm in diameter) spheroidal microstructures described in the literature has been poorly demonstrated (Schopf and Walter, 1983). Previously reported large spheres include hollow specimens, but their wall textures are often obscure (Schopf, 1993; Schopf and Packer, 1987; Ueno et al., 2006; Walsh, 1992). In the present samples, wall architecture and the spectrum of morphological variability indicate flexible, compressible and breakable physical properties.

About 10% of the spheroidal microstructures have inner bodies, sometimes attached to the wall and sometimes apparently discrete (Fig. 11c–j, l–m). Their origin is presently equivocal, as with other examples (Awramik and Barghoorn, 1977; Westall et al., 1995). Some may indicate a degree of cellular complexity. Others appear taphonomic in origin and resemble similar microstructures from microfossils in younger rocks (Sergeev et al., 1995; Sergeev, 2006).

Large spheroidal microstructures, commonly referred to as hollow because the cell walls were differentiated from cell contents (later replaced by chert matrix), have many common features such as (1) carbonaceous

composition, (2) narrow size-distribution, (3) internal texture potentially interpretable as cellular elaboration, (4) flexible, and sometimes breakable walls and (5) morphological variability attributable to taphonomy. Unlike the small spheroids, distinct colony-like aggregations of large spheroids have not been observed. Nor have features suggestive of vital function, but it is difficult to identify such features in many younger microfossils. A few spheres appear solid and are here dismissed as being abiogenic in origin. However, the vast majority of the spheres are hollow to semi-hollow (although now infilled with spherulitic chert), including some that appear solid or to have a heterogeneous interior because the proximal or distal wall remains visible but unfocused in the mid-plane of view. Early silicification of microbes, even when they are still alive (Renaut et al., 1998 and references therein), contributes to the preservation of a 'hollow' interior together with internal structures.

Based on the 'hollow' nature of the spheres, the taphonomic features visible in the walls and the presence in some cases of internal structures, a biogenic origin seems probable. It is difficult to postulate an abiogenic mode of formation for large 'hollow' spheres with walls of uniform and consistent thickness that show taphonomic degradation. We therefore regard these microstructures as being biogenic, and classify them as probable microfossils.

9.2.5. *Spindle-like microstructures*

The spindle-like microstructures are characterized by a relatively narrow size distribution (Fig. 15b). As with the spheres, there are specimens that display broken or torn walls, folded walls, wrinkles and interior spheroidal bodies. Also, like the spheres, the vast majority of the microstructures are hollow (now infilled with spherulitic chert) to semi-hollow (characterized by irregularly shaped voids), although they may appear solid when photographed at low magnifications or at high or low focus (Figs. 13b–d, 17a, Supplementary Fig. V).

In addition to the features shared with the spheroidal microstructures, the spindle-like microstructures are characterized by morphological elaborations such as the presence of a tapering equatorial flange or equatorial girdle (Fig. 15c). This sheet-like extension, which is solid and of the same density as the walls, is difficult to explain as a secondary compression or stretching of an originally spheroidal structure, because the microstructures are randomly oriented and not aligned to bedding planes or crystal growth structures (Fig. 13c, e, f; also see Fig. 12f–h caption). In addition, secondary stretching might be expected to result in less dense walls and streaking out in the stretched areas. The microstructures are apparently flexible; the proximal edge may be wavy or slightly curled (Figs. 12a–c, n–o, 13c, Supplementary Fig. IVb–d). However, the lensoid body shows little or no distortion, even when the flange is bent. It is difficult to explain how only part of a microstructure could be deformed unless it consisted of a fairly rigid spherical body, surrounded by a more flexible equatorial flange. In addition, the microstructures often occur in pairs or colony-like aggregations (Supplementary Fig. V, Fig. 13), a mode of occurrence that could be interpreted as indicating a colonial habit or even a reproductive mode, although further analysis is required to confirm this.

Numerous abiogenic modes of formation (including the biomorph model discussed above) were considered and discounted. For example, the formation of hollow spindles as fenestral structures resulting from the infilling of gas structures in a biofilm (Westall et al., 2001) is precluded by the presence of the solid flange structure and the random orientation. Formation as necked fluid inclusions (Roedder, 1984; Dutkiewicz et al., 1998) seems implausible, because some spindle-like microstructures appear broken, and they are infilled by microcrystalline quartz identical to the chert matrix. Formation as particle concentrations around crystal growth margins is ruled out because the contours of the spindle walls do not conform to the crystal margins. Growth around the margins of rare gypsum crystals (Walsh, 1992) also seems unlikely. Such pinacoid crystals might give rise to a spindle shape, but there is nothing to suggest that the microcrystalline quartz replaced gypsum, and the spindles are very consistent in shape and dimensions; crystals usually show greater variation. It is therefore difficult to suggest a plausible abiogenic process that could form similar microstructures. The combination of complex morphology, 'hollowness', and several features characteristic of taphonomic degradation are inconsistent with known abiogenic structures, but are consistent with known biogenic ones. We therefore interpret the spindle-shaped microstructures as being biogenic and highly probable microfossils. Significantly, almost identical spindle-shaped microstructures have been reported from Archaean (ca. 3.4 Ga) chert from the Barberton Greenstone Belt in South Africa and also interpreted as microfossils (Walsh, 1992).

10. Conclusions

The Farrel Quartzite at Mount Grant–Mount Goldsworthy contains a range of microfossil-like structures that we classify as pseudofossils to highly probable Archaean microfossils. The Archaean (synsedimentary,

and >ca. 2.97 Ga) age of the microstructures is evident because they are an integral part of water-sorted, sedimentary fabrics in a sedimentary rock succession. The microstructures were not introduced after deposition. There is no evidence to contradict a biogenic interpretation of the microstructures, and comparison of the microstructures to the many independently formulated criteria in Table 3 strongly supports the biogenic hypothesis. Although future research may raise alternative abiogenic hypotheses against which these microstructures may be tested, currently the most plausible explanation for their formation is biogenesis.

The morphological diversity among the Mount Grant–Mount Goldsworthy microstructures suggests that (assuming they represent Archaean organisms) a diverse array of microbes flourished in Archaean shallow-water environments by ca. 2.97 Ga. This is consistent with morphological diversity observed in Archaean stromatolites also found in the Pilbara Craton (Hofmann et al., 1999; Allwood et al., 2006), but provides actual biological remains of organisms rather than structures they may have left behind. Further studies of the Mount Grant–Mount Goldsworthy microstructures should assist in understanding early biodiversity and the antiquity of life on Earth.

Acknowledgements

We especially wish to express our gratitude to Dr. R. Sugisaki, Dr. M. Adachi, Dr. M. Hoshino, Dr. T. Matsubara, Dr. T. Nishikawa, Nagoya University for their useful comments and encouragement, and to Dr. K. Yamamoto, Nagoya University and Dr. H. Maekawa, Osaka Prefecture University for XRF and SEM-EDX analyses, respectively. KS gratefully acknowledges Mr. T. Asano for his help in sampling at Mounts Goldsworthy and Grant in 2001 and to Dr. K.J. McNamara, Western Australia Museum and the Australian Customs Service, for their assistance in exporting samples to Japan. Dr. A. Hickman (GSWA) assisted in updating the geochronological constraints. Dr. M. Brasier and an anonymous reviewer made constructive criticisms on an early version that allowed us to focus and improve the manuscript considerably. Dr. J.W. Schopf, Dr. V.N. Sergeev and an anonymous reviewer provided for helpful and constructive comments on the revised manuscript. This paper is a product of a Joint Research Program (Japan-Australia) supported by the Japan Society for the Promotion of Science. KG and MVK publish with the permission of the Director of the Geological Survey of Western Australia. MRW, CPM and AA acknowledge funding from Macquarie University and the Australian Research Council.

Appendix A. Supplementary data

Supplementary data associated with this article can be found, in the online version, at doi:10.1016/j.precamres.2007.03.006.

References

Al-Hanbali, H.S., Sowerby, S.J., Holm, N.G., 2001. Biogenicity of silicified microbes from a hydrothermal system: relevance to the search for evidence of life on earth and other planets. Earth Planet. Sci. Lett. 191, 213–218.

Allwood, A.C., Walter, M.R., Kamber, B.S., Marshall, C.P., Burch, I.W., 2006. Stromatolite reef from the Early Archaean era of Australia. Nature 441, 714–718.

Altermann, W., 2001. The oldest fossils of Africa—a brief reappraisal of reports from the Archean. J. Afr. Earth Sci. 33, 427–436.

Awramik, S.M., Barghoorn, E.S., 1977. The Gunflint microbiota. Precambrian Res. 5, 121–142.

Awramik, S.M., Schopf, J.W., Walter, M.R., 1983. Filamentous fossil bacteria from the Archean of Western Australia. Precambrian Res. 20, 357–374.

Awramik, S.M., Schopf, J.W., Walter, M.R., 1988. Carbonaceous filaments from North Pole. Western Australia: are they fossil bacteria in Archean stromatolites? A discussion. Precambrian Res. 39, 303–309.

Brasier, M.D., Green, O.R., Jephcoat, A.P., Kleppe, A.K., Van Kranendonk, M.J., Lindsy, J.F., Steele, A., Grassineau, N.V., 2002. Questioning the evidence for Earth's oldest fossils. Nature 416, 76–81.

Brasier, M.D., Green, O.R., Lindsay, J.F., McLoughlin, N., Steele, A., Stokes, C., 2005. Critical testing of Earth's oldest putative fossil assemblage from the ∼3.5 Apex chert, Chinaman Creek, Western Australia. Precambrian Res. 140, 55–102.

Brasier, M.D., Green, O.R., Lindsay, J.F., Steele, A., 2004. Earth's oldest (∼3.5 Ga) fossils and the 'Early Eden' hypothesis: questioning the evidence. Origins Life Evol. Biosphere 2004 34, 257–269.

Brasier, M., McLoughlin, N., Green, O., Wacey, D., 2006. A fresh look at the fossil evidence for early Archaean cellular life. Phil. Trans. R. Soc. B 361, 887–902.

Bucher, K., Frey, M., 1994. Petrogenesis of Metamorphic Rocks. Springer-Verlag, New York, p. 318.

Buick, R., 1984. Carbonaceous filaments from North Pole, Western Australia: are they fossil bacteria in Archaean stromatolites? Precambrian Res. 24, 157–172.

Buick, R., 1988. Carbonaceous filaments from North Pole, Western Australia: are they fossil bacteria in Archaean stromatolites? A reply. Precambrian Res. 39, 311–317.

Buick, R., 1990. Microfossil recognition in Archean rocks: an appraisal of spheroids and filaments from a 3500 M.Y. old chert-barite unit at North Pole, Western Australia. Palaios 5, 441–459.

Buick, R., Dunlop, J.S.R., 1990. Evaporitic sediments of Early Archaean age from the Warrawoona Group, North Pole, Western Australia. Sedimentology 37, 247–277.

Dunlop, J.S.R., Muir, M.D., Milne, V.A., Groves, D.I., 1978. A new microfossil assemblage from the Archaean of Western Australia. Nature 274, 676–678.

Dutkiewicz, A., Rasmussen, B., Buick, R., 1998. Oil preserved in fluid inclusions in Archaean sandstones. Nature 395, 886–888.

García-Ruiz, J.M., Hyde, S.T., Carnerup, A.M., Christy, A.G., Van Kranendonk, M.J., Welham, N.J., 2003. Self-assembled silica-carbonate structures and detection of ancient microfosils. Science 302, 1194–1197.

García-Ruiz, J.M., Carnerup, A., Christy, A.G., Welham, N.J., Hyde, S.T., 2002. Morphology: an ambiguous indicator for biogenicity. Astrobiology 2, 335–351.

Ghiorse, W.C., 1997. Subterranean life. Science 275, 789–790.

Gold, T., 1999. The Deep Hot Biosphere: The Myth of Fossil Fuels. Springer-Verlag, New York.

Grey, K., 1986. Problematic microstructures in the Discovery Chert, Bangemall Group, Western Australia—ambient grains or microfossils? Western Australia Geological Survey, Professional Papers for 1984, pp. 22–31.

Hayes, J.M., Kaplan, I.R., Wedeking, K.W., 1983. Precambrian organic geochemistry. Preservation of the record. In: Schopf, J.W. (Ed.), Earth's Earliest Biosphere, Its Origin and Evolution. Princeton University Press, Princeton, pp. 93–134.

Herdiantia, N.R., Browne, P.R.L., Rodgers, K.A., Campbell, K.A., 2000. Mineralogical and textural changes accompanying aging of silica sinter. Miner. Deposita 35, 48–62.

Herzig, P.M., Becker, K.P., Stoffers, P., Bäcker, H., Blum, N., 1988. Hydrothermal silica chimney fields in the Galapagos Spreading Center at 86°W. Earth Planet. Sci. Lett. 89, 261–272.

Hofmann, B.A., Farmer, J.D., 2000. Filamentous fabrics in low-temperature mineral assemblages: are they fossil biomarkers? Implications for the search for a subsurface fossil record on the early Earth and Mars. Planet. Space Sci. 48, 1077–1086.

Hofmann, H.J., 1971. Precambrian fossils, pseudofossils, and problematica in Canada. Geol. Surv. Can., Bull. 189, 146.

Hofmann, H.J., 1972. Precambrian remains in Canada: fossils, dubiofossils, and pseudofossils. In: International Geological Congress, 24th Session, Proceedings, Montreal, pp. 20–30.

Hofmann, H.J., 1994. Proterozoic carbonaceous compression ("metaphytes" and "worms"). In: Bengtson, S. (Ed.), Early Life on Earth. Nobel Symposium 84. Columbia University Press, New York, pp. 342–357.

Hofmann, H.J., 2004. Archean microfossils and abiomorphs. Astrobiology 4, 135–136.

Hofmann, H.J., Grey, K., Hickman, A.H., Thorpe, R.I., 1999. Origin of 3.45 Ga coniform stromatolites in Warrawoona Group, Western Australia. Geol. Soc. Am. Bull. 111, 1256–1262.

Holm, N.G., Charlou, J.L., 2001. Initial indications of abiotic formation of hydrocarbons in the Rainbow ultramafic hydrothermal system, Mid-Atlantic Ridge. Earth Planet. Sci. Lett. 191, 1–8.

Jehlicka, J., Urban, O., Pokorny, J., 2003. Raman spectroscopy of carbon and solid bitumens in sedimentary and metamorphic rocks. Spectrochim. Acta Part A 59, 2341–2352.

Kiyokawa, S., Ito, T., Ikehara, M., Kitajima, F., 2006. Middle Archean volcano-hydrothermal sequence: bacterial microfossil-bearing 3.2 Ga Dixon Island Formation, coastal Pilbara terrane, Australia. Geol. Soc. Am. Bull. 118, 3–22.

Knoll, A.H., Barghoorn, E.S., 1977. Archean microfossils showing cell division from the Swaziland system of South Africa. Science 198, 396–398.

Knoll, A.H., Barghoorn, E.S., 1974. Ambient pyrite in Precambrian chert: new evidence and a theory. Proc. Natl. Acad. Sci. USA 71, 2329–2331.

Lindsay, J.F., Brasier, M.D., McLoughlin, N., Green, O.R., Fogel, M., Steele, A., Mertzman, S.A., 2005. The problem of deep carbon—an Archean paradox. Precambrian Res. 143, 1–22.

Lowe, D.R., 1983. Restricted shallow-water sedimentation of Early Archean stromatolitic and evaporitic strata of the Strelley Pool Chert Pilbara Block Western Australia. Precambrian Res. 19, 239–283.

Lowe, D.R., 1999. Petrology and sedimentology of cherts and related silicified sedimentary rocks in the Swaziland Supergroup. Geol. Soc. Am. Spec. Paper 329, 83–114.

Marshall, C.P., Gordon, D.L., Snape, C.E., Hill, A.C., Allwood, A.C., Walter, M.R., Van Kranendonk, M.J., Bowden, S.A., Sylva, S.P., Summons, R.E., 2007. Structural characterization of kerogen in 3.4 Ga Archaean cherts from the Pilbara Craton, Western Australia. Precambrian Res. 155, 1–23.

McCollom, T.M., 2003. Formation of meteorite hydrocarbons from thermal decomposition of siderite ($FeCO_3$). Geochim. Cosmochim. Acta 67, 311–317.

McCollom, T.M., Seewald, J.S., 2006. Carbon isotope composition of organic compounds produced by abiotic synthesis under hydrothermal conditions. Earth Planet. Sci. Lett. 243, 74–84.

Moorbath, S., 2005. Dating earliest life. Nature 434, 155.

Nagy, B., Nagy, L.A., 1969. Early Pre-Cambrian Onverwacht microstructures: possibly the oldest fossils on earth? Nature 223, 1226–1229.

Nijman, W., de Bruijne, K.C.H., Valkering, M.E., 1998. Growth fault control of Early Archaean cherts, barite mounds and chert-barite veins, North Pole Dome, Eastern Pilbara, Western Australia. Precambrian Res. 88, 25–52.

Oehler, J.H., Schopf, J.W., 1971. Artificial microfossils: Experimental studies of permineralization of blue-green algae in silica. Science 174, 1229–1231.

Oehler, J.H., 1976. Hydrothermal crystallization of silica gel. Geol. Soc. Am. Bull. 87, 1143–1152.

O'Toole, G., Kaplan, H.B., Kolter, R., 2000. Biofilm formation as microbial development. Ann. Rev. Microbiol. 54, 49–79.

Rasmussen, B., 2000. Filamentous microfossils in a 3.235-million-year-old volcanogenic massive sulphide deposit. Nature 405, 676–679.

Renaut, R.W., Jones, B., Tiercelin, J.-J., 1998. Rapid in situ silicification of microbes at Loburu hot springs, Lake Bogoria, Kenya Rift Valley. Sedimentology 45, 1083–1103.

Roedder, E., 1984. Fluid inclusions. Rev. Mineral. 12, 59–77.

Schopf, J.W., 1968. Microflora of the Bitter Springs Formation, Late Precambrian, central Australia. J. Paleontol. 42, 651–688.

Schopf, J.W., 1993. Microfossils of the Early Archean Apex Chert: new evidence of antiquity of life. Science 260, 640–646.

Schopf, J.W., 2006. Fossil evidence of Archaean life. Phil. Trans. R. Soc. B 361, 869–885.

Schopf, J.W., Klein, C., 1992. The Proterozoic Biosphere, A Multidisciplinary Study. Cambridge University Press.

Schopf, J.W., Packer, B.M., 1987. Early Archean (3.3-billion to 3.5-billion-year-old) microfossils from Warrawoona Group, Australia. Science 237, 70–73.

Schopf, J.W., Walter, M.R., 1983. Archean microfossils: new evidence of ancient microbes. In: Schopf, J.W. (Ed.), Earth's Earliest Biosphere, Its Origin and Evolution. Princeton University Press, Princeton, pp. 214–239.

Schulz, H.N., Jørgensen, B.B., 2001. Big. Ann. Rev. Microbiol. 55, 105–137.

Sergeev, V.N., Knoll, A.H., Grotzinger, J.P., 1995. Paleobiology of the Mesoproterozoic Billyakh Group, Anabar Uplift, Northern Siberia. Paleontological Society, Memoir 39 (J. Paleontol. 69(Suppl. 1)), 37.

Sergeev, V.N., 2006. Precambrian Microfossils in Cherts, Their Paleobiology, Classification and Biostratigraphic Usefulness. Transactions of the Geological Institute, Geos, Moscow, p. 567.

Simonson, B.M., 1985. Sedimentology of cherts in the Early Proterozoic Wishart Formation, Quebec-Newfoundland, Canada. Sedimentology 32, 23–40.

Smithies, R.H., Van Kranendonk, M.J., Hickman, A.H., 2004. De Grey, W.A. Sheet 2757 (Version 2.0): Western Australia Geological Survey, 1:100 000 Geological Series.

Sugisaki, R., Shimomura, T., Ando, K., 1977. An automatic X-ray fluorescence method for the analysis of silicate rocks. J. Geol. Soc. Jpn. 83, 725–733.

Sugitani, K., 1992. Geochemical characteristics of Archean cherts and other sedimentary rocks in the Pilbara Block, Western Australia: evidence for Archean seawater enriched in hydrothermally-derived iron and silica. Precambrian Res. 57, 21–47.

Sugitani, K., Mimura, K., Suzuki, K., Nagamine, K., Sugisaki, R., 2003. Stratigraphy and sedimentary petrology of an Archean volcanic-sedimentary succession at Mt. Goldsworthy in the Pilbara Block. Western Australia: implications of evaporite (nahcolite) and barite deposition. Precambrian Res. 120, 55–79.

Sugitani, K., Yamamoto, K., Adachi, M., Kawabe, I., Sugisakli, R., 1998. Archean cherts derived from chemical, biogenic and clastic sedimentation in a shallow restricted basin: examples from the Gorge Creek Group in the Pilbara Block. Sedimentology 45, 1045–1062.

Sugitani, K., Nagaoka, T., Mimura, K., Grey, K., Van Kranendonk, M.J., Minami, M., Marshall, C.P., Allwood, A., Walter, M.R., 2006a. Discovery of possible microfossils from c. 3.4 Ga Strelley Pool Chert, Kelly Group, Pilbara Craton: evidence for antiquity of life and biotic diversity? Geophy. Res. Abst. 8, 02562. EGU 3rd General Assembly.

Sugitani, K., Nagaoka, T., Mimura, K., Grey, K., Van Kranendonk, M.J., Minami, M., Marshall, C.P., Allwood, A., Walter, M.R., 2006b. Possible microfossils from the ∼3.4 Ga Strelley Pool Chert, Pilbara Craton, Western Australia. International Palaeontological Congress (IPC2006) (June 17–21, 2006, at Beijing, China). Ancient Life and Modern Approaches, 269 p.

Sugitani, K., Yamashita, F., Nagaoka, T., Yamamoto, K., Minami, M., Mimura, K., Suzuki, K., 2006c. Geochemistry and sedimentary petrology of Archean clastic sedimentary rocks at Mt. Goldsworthy, Pilbara Craton, Western Australia: evidence for the early evolution of continental crust and hydrothermal alteration. Precambrian Res. 147, 124–147.

Sugitani, K., Yamashita, F., Nagaoka, T., Minami, M., Yamamoto, K., 2006d. Geochemistry of heavily altered Archean volcanic and volcaniclastic rocks of the Warrawoona Group, at Mt. Goldsworthy in the Pilbara Craton, Western Australia: implications for alteration and origin. Geochem. J. 40, 523–535.

Tice, M.M., Lowe, D.R., 2004. Photosynthetic microbial mats in the 3.416-Myr-old ocean. Nature 431, 549–552.

Tice, M.M., Lowe, D.R., 2006. The origin of carbonaceous matter in pre-3.0 Ga greenstone terrains: a review and new evidence from the 3.42 Ga Buck Reef Chert. Earth Sci. Rev. 76, 259–300.

Tyler, S.A., Barghoorn, E.S., 1963. Ambient pyrite grains in Precambrian cherts. Am. J. Sci. 261, 424–432.

Ueno, Y., Isozaki, Y., McNamara, K.J., 2006. Coccoid-like microstructures in a 3.0 Ga chert from Western Australia. Int. Geol. Rev. 48, 78–88.

Ueno, Y., Isozaki, Y., Yurimoto, H., Maruyama, S., 2001. Carbon isotopic signatures of individual Archean microfossils(?) from Western Australia. Int. Geol. Rev. 43, 196–212.

Ueno, Y., Yoshioka, H., Maruyama, S., Isozaki, Y., 2004. Carbon isotopes and petrography of kerogens in ∼3.5-Ga hydrothermal silica dykes in the North Pole area, Western Australia. Geochim. Cosmochim. Acta 68, 573–589.

Van Kranendonk, M.J., 2006. Volcanic degassing, hydrothermal circulation and the flourishing of early life on Earth: A review of the evidence from c. 3490–3240 Ma rocks of the Pilbara Supergroup, Pilbara Craton, Western Australia. Earth Sci. Rev. 74, 197–240.

Van Kranendonk, M.J., Hickman, A.H., Smithies, R.H., Williams, I.R., Bagas, L., Farrell, T.R., 2006. Revised lithostratigraphy of Archean supracrustal and intrusive rocks in the northern Pilbara Craton, Western Australia. Western Australia Geological Survey, Record 2006/15.

Van Kranendonk, M.J., Smithies, R.H., Hickman, A.H., Champion, D.C., 2007. Review: secular tectonic evolution of Archean continental crust: interplay between horizontal and vertical processes in the formation of the Pilbara Craton, Australia. Terra Nova 19, 1–38.

van Zuilen, M.A., Lepland, A., Arrhenius, G., 2002. Reassessing the evidence for the earliest traces of life. Nature 418, 627–630.

Walsh, M.M., 1992. Microfossils and possible microfossils from Early Archean Onverwacht Group, Barberton Mountain Land, South Africa. Precambrian Res. 54, 271–293.

Walsh, M.M., Lowe, D.R., 1985. Filamentous microfossils from the 3,500-Myr-old Onverwacht Group, Barberton Mountain Land, South Africa. Nature 314, 530–532.

Walter, M.R., 1996. Ancient hydrothermal ecosystems on earth: a new palaeobiological frontier. In: Bock, G.R., Goode, J.A. (Eds.), Evolution of Hydrothermal Ecosystems on Earth (and Mars?). Wiley, Chichester, pp. 112–127.

Westall, F., Boni, L., Guerzoni, E., 1995. The experimental silicification of microorganisms. Palaeontology 38, 495–528.

Westall, F., de Vries, S.T., Nijman, W., Rouchon, V., Orberger, B., Pearson, V., Verchovsky, A., Wright, I., Rouzaud, J.-N., Marchesini, D., Severine, A., 2006. The 3.466 Ga "Kitty's Gap Chert", an early Archean microbial ecosystem. Geol. Soc. Am. Bull. Spec. Paper 405, 105–131.

Westall, F., de Wit, M.J., Dann, J., van der Gaast, S., de Ronde, C.E.J., Gerneke, D., 2001. Early Archean fossil bacteria and biofilms in hydrothermally-influenced sediments from the Barberton Greenstone Belt, South Africa. Precambrian Res. 106, 93–116.

Westall, F., Folk, R.L., 2003. Exogenous carbonaceous microstructures in Early Archaean cherts and BIFs from the Isua Greenstone belt: implications for the search for life in ancient rocks. Precambrian Res. 126, 313–330.

Westall, F., Steele, A., Toporski, J., Walsh, M., Allen, C., Guidry, S., McKay, D., Gibson, E., Chafetz, H., 2000. Polymeric substances and biofilms as biomarkers in terrestrial materials: implications for extraterrestrial samples. J. Geophys. Res. 105, 24511–24527.

Wopenka, B., Pasteris, J.D., 1993. Structural characterization of kerogens to granulite-facies graphite: applicability of Raman microprobe spectroscopy. Am. Mineral. 78, 533–557.

Yui, T.-F., Huang, E., Xu, J., 1996. Raman spectrum of carbonaceous material: a possible metamorphic grade indicator for low-grade metamorphic rocks. J. Metamorph. Geol. 14, 115–124.